Marine Chemistry 257 (2023) 104324

Contents lists available at ScienceDirect

Marine Chemistry

journal homepage: www.elsevier.com/locate/marchem

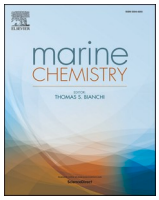

Macronutrient biogeochemistry in Antarctic land-fast sea ice: Insights from a circumpolar data compilation

Sian F. Henley [a,*], Stefano Cozzi [b], François Fripiat [c], Delphine Lannuzel [d], Daiki Nomura [e], David N. Thomas [f], Klaus M. Meiners [g,h,i], Martin Vancoppenolle [j], Kevin Arrigo [k], Jacqueline Stefels [l], Maria van Leeuwe [l], Sebastien Moreau [m], Elizabeth M. Jones [n], Agneta Fransson [m], Melissa Chierici [n], Bruno Delille [o]

[a] School of GeoSciences, University of Edinburgh, James Hutton Road, Edinburgh EH9 3FE, UK
[b] CNR-ISMAR, Istituto di Scienze Marine, Area di Ricerca di Basovizza, Edificio Q2. SS14, km 163,5, 34149 Trieste, Italy
[c] Department of Geosciences, Environment and Society, Université Libre de Bruxelles, Brussels, Belgium
[d] Institute for Marine and Antarctic Studies, University of Tasmania, 20 Castray Esplanade, Hobart TAS 7001, Australia
[e] Hokkaido University, Hakodate, Japan
[f] Faculty of Biological & Environmental Sciences, University of Helsinki, Finland
[g] Australian Antarctic Division, Department of Climate Change, Energy, the Environment and Water, Kingston, Tasmania, Australia
[h] Australian Antarctic Program Partnership, Institute for Marine and Antarctic Studies, University of Tasmania, Hobart, Tasmania, Australia
[i] Australian Centre for Excellence in Antarctic Science, University of Tasmania, Hobart, Tasmania, Australia
[j] Sorbonne Université, LOCEAN-IPSL, CNRS/IRD/MNHN, Paris, France
[k] Department of Earth System Science, 473 Via Ortega, Room 141, Stanford University, Stanford, CA 94305-4216, USA
[l] University of Groningen Groningen Institute for Evolutionary Life Sciences (GELIFeS), PO Box 11103 9700 CC, Groningen, the Netherlands
[m] Norwegian Polar Institute, Fram Centre, Tromsø, Norway
[n] Institute of Marine Research, Fram Centre, 9007 Tromsø, Norway
[o] Chemical Oceanography Unit, Freshwater and Oceanic Sciences Unit of Research, University of Liège, Belgium

ARTICLE INFO

Keywords:
Nutrients
Sea ice
Antarctica
Nitrogen cycle
Ice algae
Primary production
Remineralisation
Organic matter

ABSTRACT

Antarctic sea ice plays an important role in Southern Ocean biogeochemistry and mediating Earth's climate system. Yet our understanding of biogeochemical cycling in sea ice is limited by the availability of relevant data over sufficient temporal and spatial scales. Here we present a new publicly available compilation of macronutrient concentration data from Antarctic land-fast sea ice, covering the full seasonal cycle using datasets from around Antarctica, as well as a smaller dataset of macronutrient concentrations in adjacent seawater. We show a strong seasonal cycle whereby nutrient concentrations are high during autumn and winter, due to supply from underlying surface waters, and then are utilised in spring and summer by mixed ice algal communities consisting of diatoms and non-siliceous species. Our data indicate some degree of nutrient limitation of ice algal primary production, with silicon limitation likely being most prevalent, although uncertainties remain around the affinities of sea-ice algae for each nutrient. Remineralisation of organic matter and nutrient recycling drive substantial accumulations of inorganic nitrogen, phosphate and to a lesser extent silicic acid in some ice cores to concentrations far in excess of those in surface waters. Nutrient supply to fast ice is enhanced by brine convection, platelet ice accumulation and incorporation into the ice matrix, and under-ice tidal currents, whilst nutrient adsorption to sea-ice surfaces, formation of biofilms, and abiotic mineral precipitation and dissolution can also influence fast-ice nutrient cycling. Concentrations of nitrate, ammonium and silicic acid were generally higher in fast ice than reported for Antarctic pack ice, and this may support the typically observed higher algal biomass in fast-ice environments.

* Corresponding author.
E-mail address: s.f.henley@ed.ac.uk (S.F. Henley).

https://doi.org/10.1016/j.marchem.2023.104324
Received 17 January 2023; Received in revised form 14 September 2023; Accepted 28 September 2023
Available online 7 October 2023

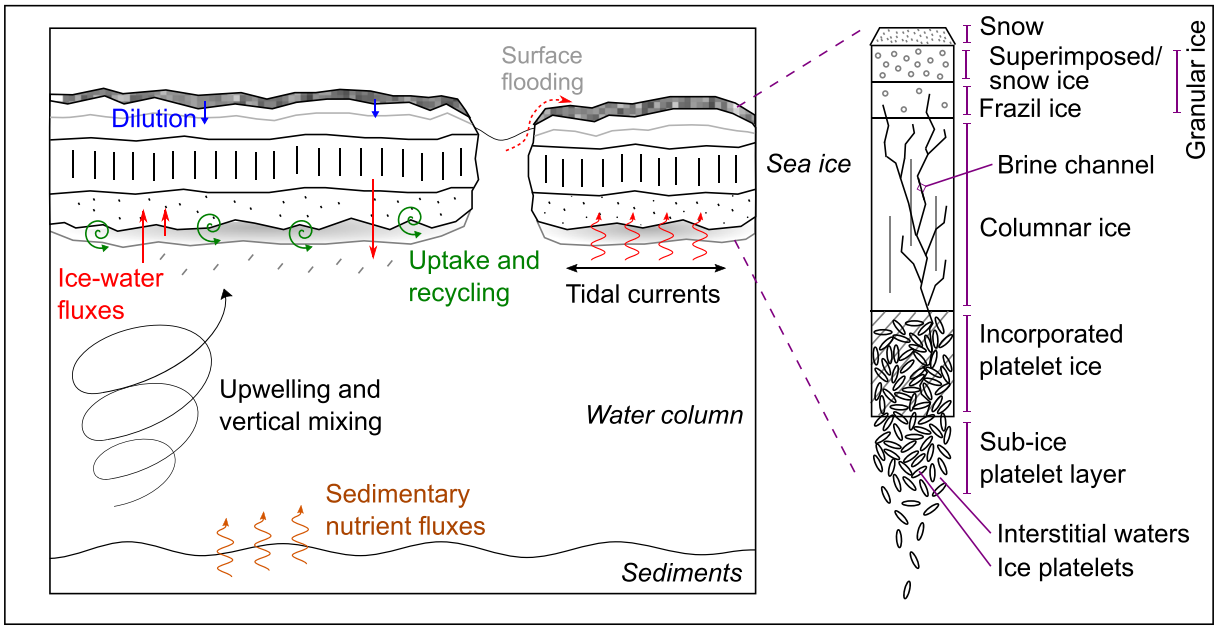

Graphical abstract: Schematic diagram showing the composition of the ice system, its position within the wider ocean system in Antarctic shelf environments, a zoomed-in image of the ice structure, and the major nutrient fluxes and processes described in this work. Major processes and fluxes are colour-coded and shown by arrows with solid lines. Processes found to play a more minor role in our dataset are shown by arrows with dotted lines and grey text.

1. Introduction

1.1. Importance of the Southern Ocean and Antarctic sea ice

The Southern Ocean plays a critical role in Earth's climate system by removing up to 50% of the total atmospheric CO_2 and up to 75% of the total heat that has been absorbed by the oceans globally (Caldeira and Duffy, 2000; DeVries, 2014; Fletcher et al., 2006; Friedlingstein et al., 2022; Frölicher et al., 2015; Orr et al., 2001). Antarctic sea ice plays an important role in mediating the exchange of both CO_2 and heat between the Southern Ocean and the atmosphere, through both physical and biogeochemical mechanisms (Delille et al., 2014; Fransson et al., 2011; Gordon, 1981). The Southern Ocean is also fundamentally important in the global ocean circulation (Marshall and Speer, 2012) and the redistribution of nutrients to the major ocean basins north of 30°S (Henley et al., 2020), with estimates suggesting that nutrients sourced from the Southern Ocean contribute over 60% of the nutrient pool in low-latitude regions (Fripiat et al., 2021; Sarmiento et al., 2004). Antarctic sea-ice dynamics also impact ocean mixing and circulation (Abernathey et al., 2016; Pellichero et al., 2018; Pellichero et al., 2017), and biogeochemical exchanges with Antarctic sea ice can alter water column inventories of nutrients and subsequent export to more northerly latitudes (Moore et al., 2018).

Despite the documented importance of Antarctic sea ice, few datasets are available to quantify associated biogeochemical processes and their influence on regional biogeochemistry, ecosystem functioning and ocean-climate feedbacks at the circumpolar scale (Fripiat et al., 2017; Lannuzel et al., 2016b; Meiners et al., 2018; Meiners et al., 2012; van Leeuwe et al., 2018). This sparsity of data limits our ability to model Antarctic marine ecosystems in and around the sea-ice zone and the underpinning biogeochemical processes. Furthermore, Antarctic sea ice has experienced unprecedented reductions in extent since 2014 (Eayrs et al., 2021; Parkinson, 2019), with the most recent seasonal minimum extent in February 2023 being the lowest on record (United States National Snow and Ice Data Center, 2023, URL: https://nsidc.org/arcticseaicenews/sea-ice-tools/). Fast-ice extent has shown a similar pattern of decline over the same time period with the lowest recorded extent published so far being in 2022 (Fraser et al., 2023). These observed changes make it all the more urgent to significantly improve our understanding of these systems and therefore our ability to predict the impacts of ongoing and anticipated climate change. Here, we focus on the macronutrients nitrate, nitrite, ammonium, phosphate and silicic acid in Antarctic land-fast sea ice and underlying waters to provide the circumpolar data coverage required to drive a step-change in our understanding of this important component of the coastal Southern Ocean ecosystem.

1.2. Dynamics and importance of Antarctic land-fast sea ice

Land-fast sea ice (hereafter fast ice) is annual or multi-year sea ice attached to shorelines, shallow sea floors, ice shelf fronts, glacier tongues or grounded icebergs. It contrasts with pack ice, which drifts with prevailing ocean surface currents and winds. Growth of fast ice is strongly influenced by meteorological conditions and interactions with the surrounding marine waters (Arndt et al., 2020; Bluhm et al., 2017; Heil, 2006; Heil et al., 1996; Massom et al., 2010; Murphy et al., 1995).

Fast-ice extent varies seasonally and interannually around the Antarctic continent (221 to 601 $\times$ 10^3 km^2 in 2000–2018), accounting for 3.2–8.5% of the total Antarctic sea-ice extent between winter and summer (Fraser et al., 2021; Fraser et al., 2020; Li et al., 2020). The growth of fast ice begins in coastal waters characterised by turbulent mixing with the freezing of seawater to form frazil ice crystals. Subsequent thermodynamic thickening of the ice occurs due to the formation of columnar ice on the bottom of the solid ice, as well as the accumulation of snow and associated formation of snow ice or superimposed ice on the surface (McGuinness et al., 2009; Rees Jones and Wells, 2018; Tang et al., 2007). In some areas, the transport of super-cooled plumes of ice shelf water leads to the formation of platelet ice, which may accumulate under the fast ice forming a sub-ice platelet layer, and/or consolidate into existing fast ice forming incorporated platelet ice (Hoppmann et al., 2020). These platelet-ice layers are characterised by variable spatial patterns and temporal evolutions (Arndt et al., 2020; Hoppmann et al., 2020). A schematic diagram of fast-ice structure is provided in the graphical abstract. Overall, the duration, thickness and physical characteristics of fast ice are the result of contrasting effects of the intensity and persistence of atmospheric cooling in autumn and

winter, snow deposition, and the occurrence of sea-ice breakout events caused by storms, extreme katabatic winds from the Antarctic continent, coastal currents, tides, or upwelling of warm water that melts the sea ice (Cozzi, 2014; Heil, 2006; Rusciano et al., 2013). Whilst there are many similarities between Antarctic fast ice and its Arctic counterpart, there are significant differences in terms of the attachment mechanisms of fast ice to coastlines, shallow seafloors and land-derived ice, the formation processes for snow ice and platelet ice (as well as the severe lack of observations of platelet ice in the Arctic), and the important role of melt ponds in Arctic fast-ice decay, which are rarely observed in Antarctica (Fraser et al., 2023; Hoppmann et al., 2020). These physical differences are very likely to lead to differences in fast-ice biogeochemistry between the two polar regions. However, the focus of our study is on nutrient cycling in Antarctic fast-ice environments.

The heterogeneous physical characteristics of Antarctic fast ice make the ice and sub-ice platelet layer refuges suitable for the growth of assemblages of autotrophic and heterotrophic organisms, ranging in size from viruses to copepods, which spend all or part of their life cycles in sea ice (Arrigo, 2014; Bluhm et al., 2017; Horner et al., 1992; Schnack-Schiel et al., 2001). Microalgae form taxonomically distinct communities in the interior and bottom layers of fast ice, as well as in the sub-ice platelet layer (Arrigo and Thomas, 2004). Their growth in the brine-channel network within the sea-ice matrix is limited by light, as well as the low volume of the liquid phase, low temperatures and high salinities, and restricted supply of nutrients from the water column underneath (Meiners et al., 2018). In contrast, bottom ice and sub-ice platelet layers are the most biologically productive, due to their more favourable temperature and salinity conditions and proximity to seawater nutrients (Arrigo et al., 1995; Gillies et al., 2013; Guglielmo et al., 2004; Günther and Dieckmann, 1999; Ichinomiya et al., 2007; Paterson and Laybourn-Parry, 2012; Saggiomo et al., 2017). Dissolved and particulate constituents are exchanged with the surrounding coastal waters, with an increase in particulate fluxes towards the pelagic and benthic compartments during summer, when ablation of the sub-ice platelet layer and bottom ice and the break-out of fast ice take place (Cozzi and Cantoni, 2011; Pieńkowski et al., 2009; Riaux-Gobin et al., 2003; Thomas et al., 2001; Thrush et al., 2006; Zhang et al., 2014).

The availability and cycling of dissolved inorganic nutrients in Antarctic fast ice is affected by both physical and biological processes. Most nutrients are rejected through brine channels into the water column as sea ice forms, with major changes that are proportional to changes in salinity. Subsequently, nutrient concentrations can oscillate and be replenished in the bottom ice and sub-ice platelet layers because of brine convective processes during the desalination of sea ice and changes in the hydrostatic equilibrium between sea-ice brine and seawater induced by changes in air temperature, air pressure, marine currents and tides (Ackley and Sullivan, 1994; Arrigo et al., 1995; Cozzi, 2014; Fripiat et al., 2015; Gleitz et al., 1995; Lei et al., 2010; Lieblappen et al., 2018; Roukaerts et al., 2021).

From a biological point of view, the nutrients are a source of essential elements like nitrogen and phosphorus, which are assimilated by sympagic (ice-associated) microorganisms because of their role in nutrition, growth and metabolism of cells. Siliceous phytoplankton species (mainly diatoms) can also contribute substantially to primary production in fast ice (Horner et al., 1992; van Leeuwe et al., 2022; van Leeuwe et al., 2018), such that the availability of silicic acid has also been investigated as a potentially limiting factor in this habitat (Fripiat et al., 2007; Lim et al., 2019). Biological processes often cause extreme increases in nutrient concentrations in fast ice compared to their levels in seawater, as a result of high levels of nutrients being accumulated into biomass and subsequent bacterial remineralisation of particulate and dissolved organic matter, cellular release, excretion and sloppy feeding by zooplankton grazers (Arrigo, 2014; Fripiat et al., 2015; Gradinger and Ikavalko, 1998; Guglielmo et al., 2004; Horner et al., 1992; Roukaerts et al., 2021; Thomas and Dieckmann, 2002).

Table 1
Number of ice cores by month, location around Antarctica (Longitude), range of ice thickness and ice type (age).

Month	# cores	Longitude	Ice thickness	Ice type/age
April	9	69°W – 142°E	0.23–0.75 m	9 first-year ice
May	9	69°W – 142°E	0.27–0.89 m	9 first-year ice
June	8	69°W – 142°E	0.34–0.91 m	8 first-year ice
July	14	69°W – 142°E	0.25–1.18 m	14 first-year ice
August	15	69°W – 142°E	0.27–1.30 m	15 first-year ice
September	19	69°W – 167°E	0.43–1.51 m	19 first-year ice
October	22	69°W – 167°E	0.70–1.70 m	22 first-year ice
November	93	69°W – 173°E	0.70–2.60 m	93 first-year ice
December	37	69°W – 169°E	0.60–3.25 m	37 first-year ice
January	16	69°W – 166°E	1.44–1.72 m	4 first-year ice
			1.52 m	1 second-year ice
			1.52–7.00 m	11 multi-year ice
February	2	38°E – 40°E	1.32 m	1 first-year ice
			4.30 m	1 multi-year ice
March	1	141°E	0.47 m	1 first-year ice

1.3. Knowledge gaps and aims of this study

Over the past half-century, an increasing number of studies on nutrient dynamics in Antarctic fast-ice systems have been carried out. However, they have almost always been restricted to spatially-limited field campaigns, and mostly with short temporal coverage. As such, they provide environmental information that is not adequate to support large-scale modelling of Antarctic coastal ecosystems. In this study, we perform the first compilation and analysis of macronutrient concentration data for Antarctic fast ice at the circumpolar scale, using published and unpublished data. This analysis will pave the way for a better implementation of biogeochemical models in coastal sea-ice ecosystems and improve our ability to project future changes in this climatically sensitive system.

2. Materials and methods

2.1. Study areas and data coverage

Macronutrient concentration data (nitrate, nitrite, ammonium, phosphate and silicic acid) from 245 ice cores taken from fast ice around Antarctica were compiled into an open-access database hosted by the Australian Antarctic Data Centre (URL: https://data.aad.gov.au/metadata/BEPSII_2023_Fast_Ice_Nutrients). Ice cores are summarised by their seasonal coverage in Table 1 and by sampling location with information on data contributors and relevant publications in the Supplementary Information (Table S1). By Southern Ocean region, 21 cores were from the Indian Sector, 70 from the West Pacific Sector, 67 from the Ross Sea, 85 from the West Antarctic Peninsula (WAP), and 2 from the Weddell Gyre (Fig. 1).

Ice cores were collected between 1997 and 2021. Sampling effort was highest in November ($n = 93$ cores), followed by December ($n = 37$) and October ($n = 22$), with fewer than 20 cores being available for all other months and fewer than 10 per month from February to June (Table 1). Of these, 232 cores were from first-year ice, 12 cores were from multi-year ice and 1 was from second-year ice. For analyses of monthly median values for first-year ice, months with fewer than four cores were excluded.

Data were contextualised using observations of sea-ice properties taken at the time of sampling, including ice thickness, texture, structure, age and salinity, snow thickness, and freeboard level. Ice thickness was generally determined from the length of ice cores extracted. On a small number of occasions, when full ice cores could not be extracted from thick multi-year ice, ice thickness was estimated using an EM Bird electromagnetic-induction system (Sahashi et al., 2022).

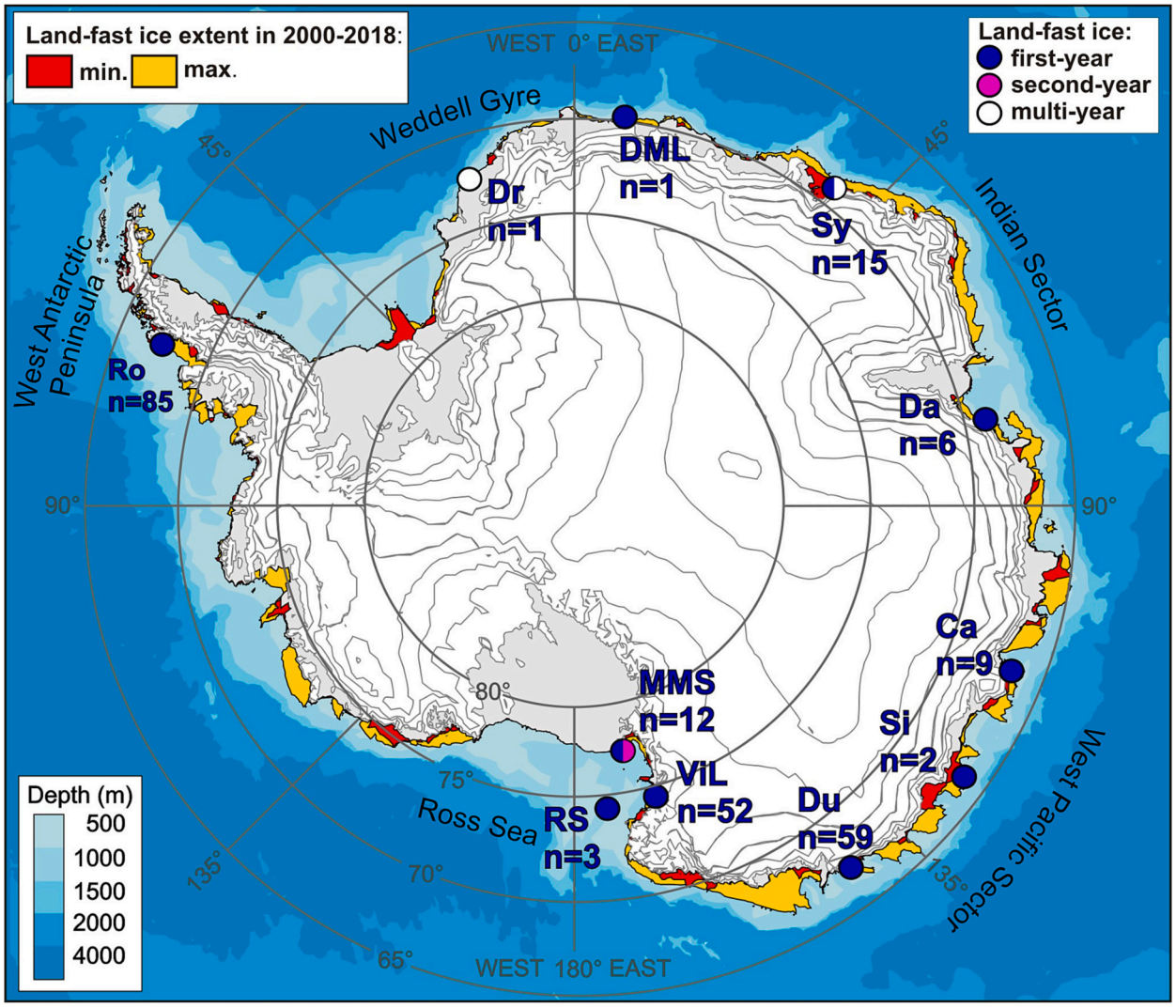

Fig. 1. Map of Antarctica showing locations of fast ice studies and the number of ice cores collected in each location. Minimum and maximum fast-ice extents from 2000 to 2018 are shown (Fraser et al., 2020), and blue shading depicts ocean bathymetry (ETOPO 5, US National Oceanic and Atmospheric Administration), as per legends. Elevation of the Antarctic continent is from the Reference Elevation Model of Antarctica (REMA) from the University of Minnesota (https://www.pgc.umn.edu/data/rema/). Sampling locations in order from Greenwich Meridian are Dronning Maud Land (DML), Syowa Station (Sy), Davis Station (Da), Casey Station (Ca), SIPEX (Si; RSV Aurora Australis), Dumont D'Urville Station (Du), three locations in the Ross Sea (Victoria Land coast (ViL), McMurdo Sound (MMS) and open Ross Sea (RS)), Rothera Station (Ro), and Drescher Inlet (Dr). Colours of circles for each location indicate the ages of fast ice from which cores were collected, as per legend, and numbers of cores from each ice type are given in Table 1. (For interpretation of the references to colour in this figure legend, the reader is referred to the web version of this article.)

Samples of under-ice water ($n = 120$) and sub-ice platelet layer ice and interstitial water ($n = 111$) were collected in some studies and are included where available. Sub-ice platelet layer ice and interstitial water were collected from core holes and cracks in the ice at Drescher Inlet and in Terra Nova Bay, Wood Bay, and Lady Newnes Bay along the Victoria Land coast in the eastern Ross Sea. Nutrient concentrations were measured in unconsolidated platelets that were sieved and melted, in interstitial waters that were separated by sieving or filtration, and in mixtures of platelets and interstitial waters that were not separated. These are handled separately in this analysis and sub-ice platelet layer ice is referred to as platelet ice for simplicity, as we do not discuss incorporated platelet ice specifically.

2.2. Comparison of field and laboratory methods and data processing

Sampling methods and laboratory analyses used in each area of interest were compared to exclude systematic biases in the analysis of the dataset. Most of the concentrations presented here were measured as bulk nutrient concentrations of melted ice core sections ($n = 1914$). Cores were collected from fast ice using ice corers (0.09 to 0.14 m diameter) and cut into sections of lengths ranging from 0.05 to 0.75 m (mean 0.15 m, median 0.12 m). Sections were cut using clean stainless-steel saws and then melted in the dark at ambient temperature or $\leq 4\,^{\circ}C$. A small number of measurements are from sea-ice brine samples, obtained by centrifugation of ice core sections (lengths 0.20 to 0.75 m, mean 0.34 m, median 0.30 m, $n = 22$; Arrigo et al., 2003). There has been concern that the change in salinity during ice core melting may cause release of intracellular nutrients into solution due to osmotic stress or shock to sea-ice microbial communities and subsequent cell lysis. Whilst we do not assess these effects directly in this study, Fripiat et al. (2017) showed that the contribution of intracellular nutrients from algal cells to nutrient concentrations measured in Antarctic pack ice should be minimal. This has also been discussed for extremely rich biological assemblages in multi-year ice (Roukaerts et al., 2021; Thomas et al., 1998) and a study comparing different melting treatments on nutrient concentrations (Roukaerts et al., 2019). However, additional studies are

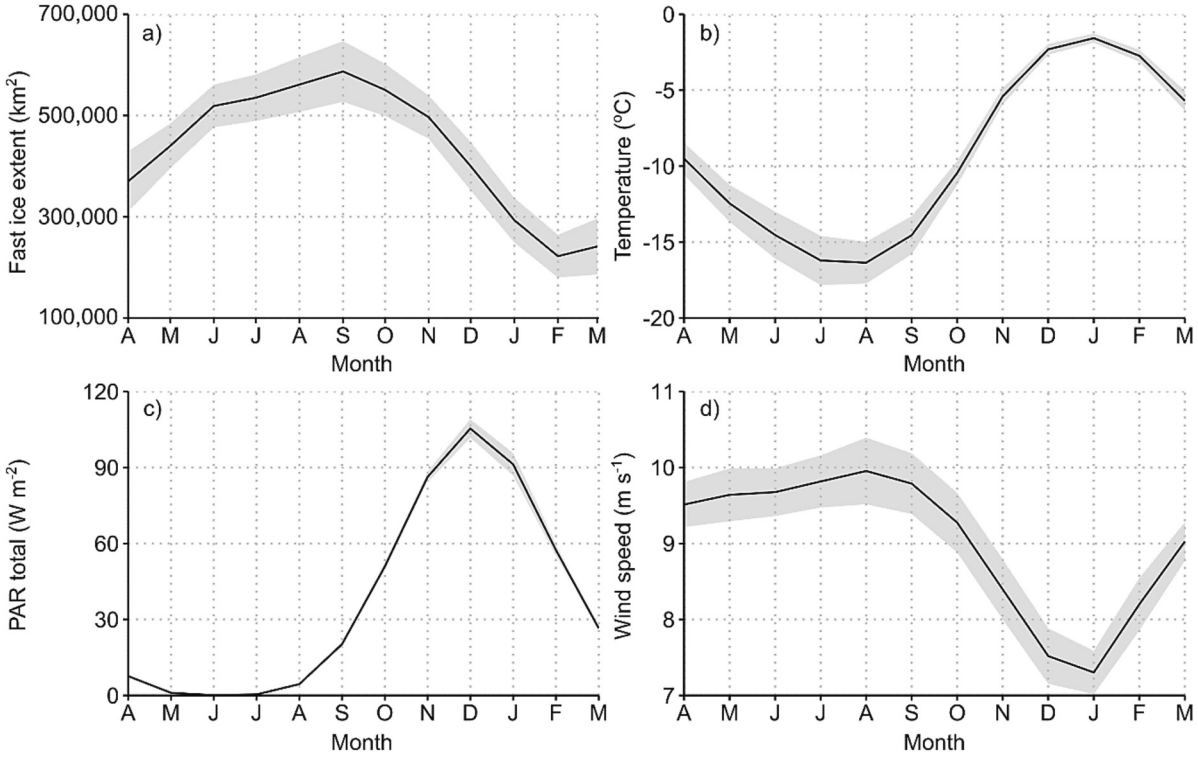

Fig. 2. Seasonal patterns of Antarctic fast-ice extent and atmospheric conditions that influence fast ice. (a) Climatology of total fast-ice extent showing monthly mean (black lines) and standard deviation (grey shading) values, March 2000 to March 2018 (Fraser et al., 2020, 2021). Also shown are monthly mean (black lines) and standard deviation (grey shading) values for (b) air temperature at 10 m height, (c) total surface downwelling PAR, and (d) surface wind speed, all averaged over the circumpolar ocean region between the Antarctic coastline and latitude 64°S, for 1980–2020, from the MERRA v2 models (Gelaro et al., 2017).

required to evaluate this effect, including measurements of the intracellular nutrient storage in sea-ice algae, which has been shown to be important in other nutrient-rich ecosystems and biofilms (e.g., Stief et al., 2022).

Nutrient concentrations were measured in filtered and unfiltered samples, either in laboratories on Antarctic research stations/ships shortly after melting or centrifugation, or in home laboratories following storage at ≤ -18 °C or by fixing with mercuric chloride and refrigeration at ≤ 4 °C. No significant differences have been reported between samples for nitrate, nitrite or phosphate stored frozen or fixed and those analysed immediately (Dore et al., 1996; Kattner, 1999). Ammonium concentrations are subject to uncertainty associated with both freezing and fixing, although no significant changes during storage have been reported between filtered and unfiltered samples (Dore et al., 1996; Fawcett et al., 2014; Kattner, 1999; Macdonald et al., 1986). Underestimation of silicic acid concentrations driven by formation of secondary silicate precipitates during freezing was reduced as far as possible in this dataset by thawing samples over a prolonged period (>24 h) or using a water bath at 50 °C, in line with recommended procedures (Becker et al., 2020; Dore et al., 1996; Sakamoto et al., 1990).

The nutrient concentrations in this compilation are mostly from automated or manual colorimetric analysis (e.g., Hydes et al., 2010). Some studies analysed ammonium (NH_4^+) concentrations using orthophthaldialdehyde (OPA) and fluorometry (Holmes et al., 1999). Specific analytical protocols varied across studies, but in general calibration standards were prepared using artificial seawater or low-nutrient seawater with salinities similar to the samples being analysed to avoid matrix effects. In this compilation, total soluble reactive phosphorus is referred to as phosphate (PO_4^{3-}) and total dissolved silicon is referred to as silicic acid ($Si(OH)_4$). Nitrite data are included where available ($n = 188$). Because nitrite data are not available for over a fifth of cores ($n = 57$), we use nitrate+nitrite ($NO_3^- + NO_2^-$) for all cores and refer to these concentrations as nitrate for simplicity. This approach is reasonable given the small and relatively constant contribution of nitrite to the nitrate+nitrite pool (median contribution of 2% across the dataset).

Data and supporting metadata were contributed from across the international scientific community working in Antarctic sea-ice biogeochemistry in .csv format and compiled into a master dataset. Further processing, manipulation and visualisation of the data was conducted in RStudio version 3.5.1 and Matlab R2018b. Nutrient concentrations are examined as a function of time, normalised ice core depth (% of ice thickness), and longitude to investigate the temporal and spatial variability of nutrient dynamics in fast ice and their exchange with surface waters. Nutrient concentrations are bulk measured values unless otherwise stated. In addition, to examine seasonal changes driven by biological processes, independent of physical changes in sea-ice properties, we normalised the nutrient concentrations measured in fast ice to a representative salinity value for the underlying seawater (34.3) according to Eq. 1, following Gleitz et al. (1995).

$$C^* = C \times (S_w/S) \quad (1)$$

C^* is the salinity-normalised nutrient concentration, C is the measured (bulk) nutrient concentration, S_w is the salinity of the underlying seawater, and S is the bulk salinity of the sea-ice sample. Sea-ice salinity was typically measured using a conductivity meter with precision ranging from 0.01 to 0.1.

2.3. Additional data

Mean concentrations of the nutrients in coastal waters surrounding fast ice were obtained for all areas of interest by reviewing the available scientific literature relevant to coastal sites around Antarctica. This allows us to examine the seasonal and spatial variability in water column nutrient dynamics and their implications for nutrient enrichment processes during the growth of fast ice and subsequent exchange between

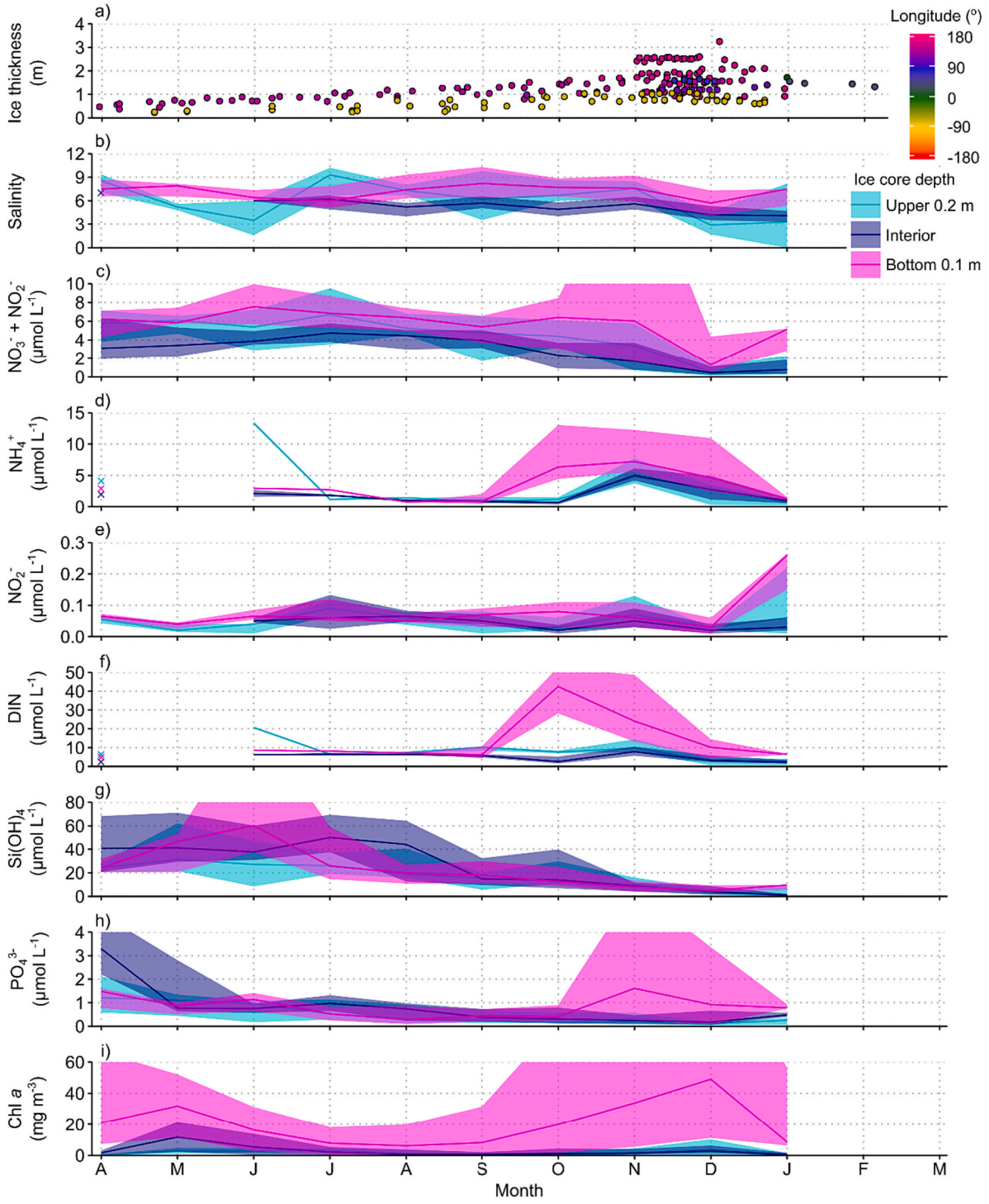

Fig. 3. Time series for first-year Antarctic fast ice of (a) ice thickness, (b) measured salinity, bulk nutrient concentrations (c) nitrate, (d) ammonium, (e) nitrite, (f) DIN, (g) silicic acid, (h) phosphate, and (i) bulk chlorophyll *a* concentration. In (a), data points are coloured by longitude according to the legend. In (b)-(h), data are binned by calendar month and shown by ice core depth (where light blue = upper 0.2 m, dark blue = interior, magenta = bottom 0.1 m), with lines connecting monthly median values and shaded areas showing interquartile ranges. x symbols are used in (b), (d) and (f) to indicate monthly median values where no value is available for the previous or following month, with colours indicating core depth. Monthly median values for February and March are excluded due to only one profile being available for each month. Chlorophyll *a* concentration data are from the AFIAC dataset (Meiners et al., 2018), binned and shown as per the salinity and nutrient data in (b)-(h). (For interpretation of the references to colour in this figure legend, the reader is referred to the web version of this article.)

ice and underlying waters. These data are summarised in the Supplementary Information (Table S2 with references).

Monthly time series of air temperature (°C) at 10 m height, surface wind speed (m s^{-1}), and total (diffuse + direct) surface downwelling photosynthetically-active radiation (PAR; W m^{-2}), estimated by MERRA v2 models for 1980–2020 (Gelaro et al., 2017), were obtained from the Giovanni Online Data System developed and maintained by NASA GES DISC (URL: https://giovanni.gsfc.nasa.gov/giovanni/). These data were averaged over the circumpolar ocean region between the Antarctic coastline and latitude 64°S, as the region in which almost all fast ice

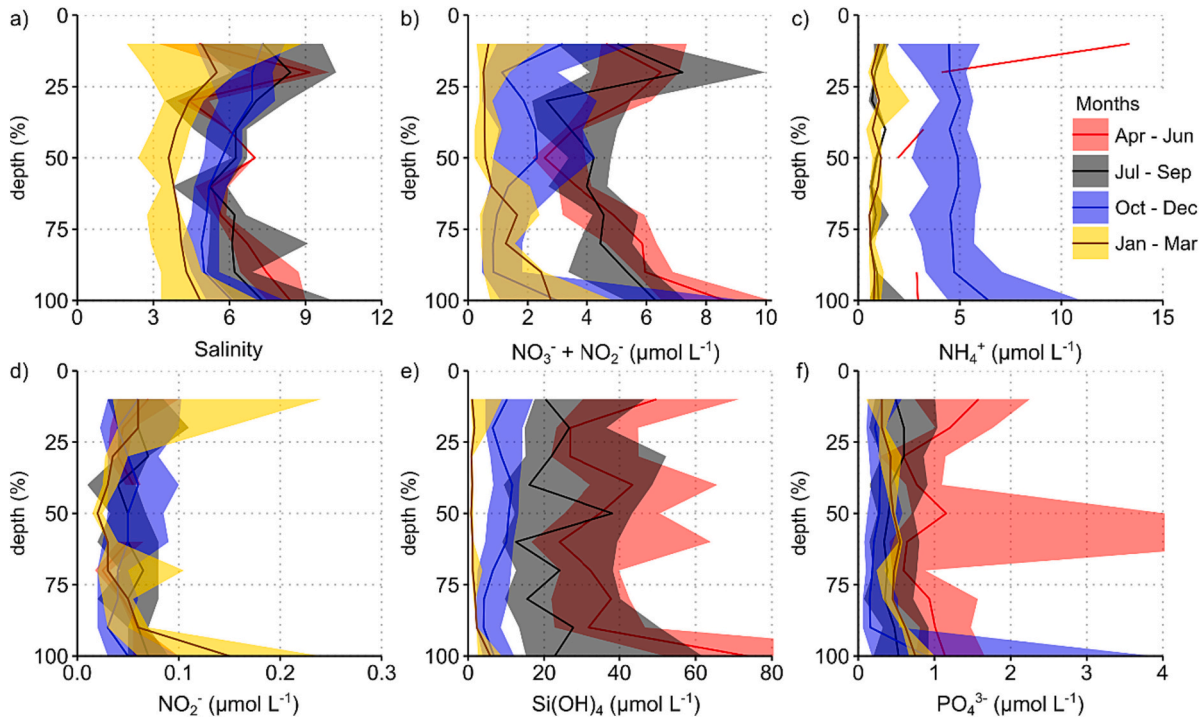

Fig. 4. Vertical profiles for bulk salinity and nutrient concentrations in first-year fast ice cores as a function of normalised ice core depth. Data are presented as seasonal averages per three months, where red = AMJ, black = JAS, blue = OND, and gold = JFM (as per legend). Median values and interquartile ranges are shown for (a) salinity, (b) nitrate, (c) ammonium, (d) nitrite, (e) silicic acid and (f) phosphate in bins of 10% of normalised core depth. (For interpretation of the references to colour in this figure legend, the reader is referred to the web version of this article.)

occurs (Fig. 1). A seasonal climatology of total fast-ice extent (Fraser et al., 2021) is shown for comparison and to contextualise the observational data presented in this compilation. We also use chlorophyll *a* concentration data from the Antarctic fast-ice algal chlorophyll *a* dataset (AFIAC; Meiners et al., 2018) to provide the biological context for interpreting the nutrient data.

3. Results

3.1. Seasonal variation in fast-ice extent and relevant atmospheric conditions

Seasonal variability in Antarctic fast-ice extent and the most relevant atmospheric conditions influencing fast ice are shown in Fig. 2. Fast-ice extent increases rapidly from April to June and then at a slower rate to its annual peak around 600,000 km^2 in late September (Fig. 2a). Fast ice then decreases from October to its annual minimum around 210,000 km^2 in February/March. Variance is evident in all months (SD >41,000 km^2), but greatest in March/April and August/September (SD >53,000 km^2), reflecting interannual variability throughout the seasonal cycle, but being largest in autumn/early winter and late winter. Air temperature at 10 m height above sea level decreases rapidly from April to minimum values below −15 °C in July and August when solar radiation is minimal (Fig. 2b). Temperature increases rapidly as the sun returns to the high southern latitudes and reaches its maximum values of −1.6 ± 0.3 °C in January. Variance is greater in July and August (SD = 1.6 °C and 1.4 °C, respectively) than in January, reflecting larger interannual variability in winter than in summer. Total PAR shows a similar seasonal pattern that also reflects that of solar radiation, with low values between April and August and zero values across the latitudinal range in June and July (Fig. 2c). PAR increases rapidly through spring and early summer in line with increasing solar radiation to a maximum of 105 ± 4 W m^{-2} in December, before decreasing again through late summer and autumn. Surface wind speed shows a different, yet still pronounced, seasonal cycle, increasing rapidly through late summer and early autumn to values over 9 m s^{-1} by April (Fig. 2d). These high values are then maintained through autumn and winter with maximum monthly mean values occurring in August (9.95 ± 0.44 m s^{-1}). Wind speed decreases through spring and summer to a seasonal minimum of 7.30 ± 0.30 m s^{-1} in January.

3.2. Seasonal variation in fast-ice physical properties: Ice thickness and salinity

Across the dataset, fast-ice thickness was minimal in early autumn as it began to form from freezing seawater (Fig. 3a). Thickness increased gradually over winter, reaching a maximum in November–December before decreasing rapidly as solar warming and strong winds caused ice melting, thinning, break-out and loss. Exceptions to this were in the multi-year fast ice at Syowa Station (Lützow-Holm Bay, East Antarctica), where ice thickness of over 4 m was observed in January and February (multi-year ice not shown in Fig. 3a). Multi-year ice was also observed at Drescher Inlet (Weddell Sea), with a thickness of 2.2 m in January. The maximum thickness of first-year ice was up to 3.3 m in the Ross Sea (indicating ice rafting), 1.7 m around East Antarctica, and 1.1 m in west Antarctica.

Sea-ice bulk salinity showed a seasonal cycle with relatively high values in upper (median 8.6), interior (median 7.0) and bottom (median 7.5) ice layers when ice was forming in April (Fig. 3b). Over winter, salinity was most variable in upper ice layers (median 3.5–9.3). Salinity showed a gradual reduction in interior ice layers to a minimum of 4.1 in January. Salinity was higher in bottom ice layers than in interior ice over the full seasonal cycle, with a maximum median value of 8.2 in September decreasing to a minimum of 5.7 in December. The seasonal minimum salinity in upper ice layers also occurred in December (median 2.9), after a pronounced reduction from the November value (7.6). Median salinity values in both bottom and upper ice layers increased again from December to January. Seasonal profiles of ice-core salinity

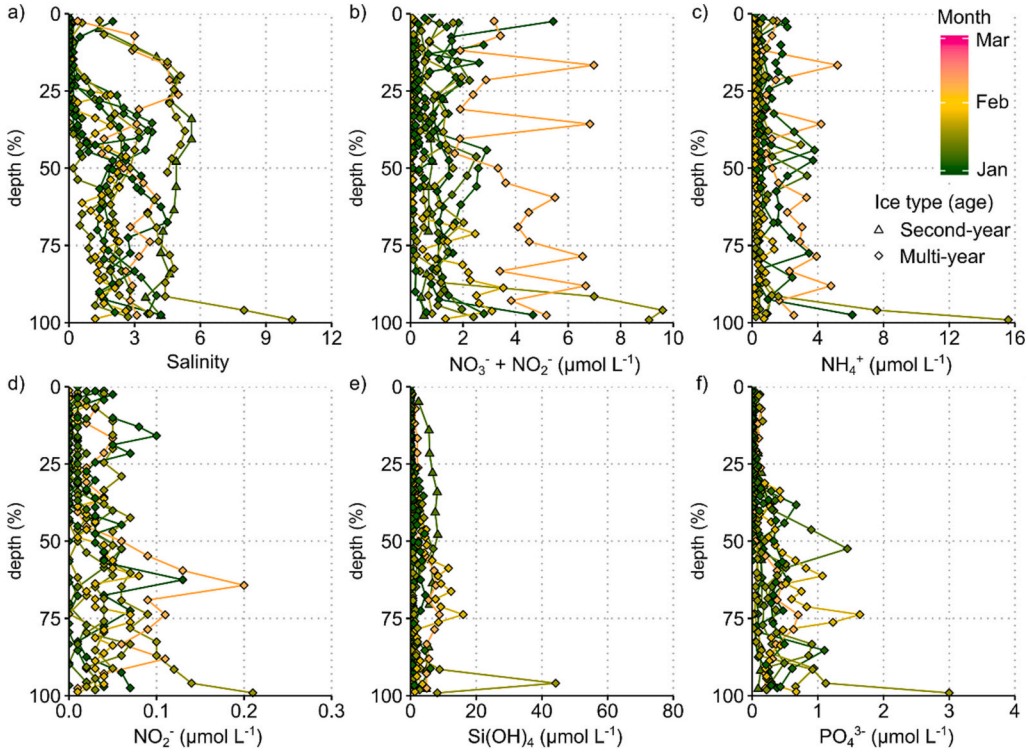

Fig. 5. Vertical profiles for bulk salinity and nutrient concentrations in multi-year fast ice cores as a function of normalised ice core depth. Shown are measured values of (a) salinity, (b) nitrate, (c) ammonium, (d) nitrite, (e) silicic acid and (f) phosphate. Data are colour-coded by sampling date from 1 January (dark green) to mid-February (orange), as per legend. Symbol type depicts ice type, where triangle = second-year ($n = 1$, Ross Sea) and diamond = multi-year ($n = 12$, Syowa Station and Drescher Inlet). (For interpretation of the references to colour in this figure legend, the reader is referred to the web version of this article.)

over the full ice thickness (Fig. 4a) showed a characteristic C-shape in autumn and winter, albeit with some small-scale variability. C-shaped profiles became more pronounced overall through spring and into summer when they were most pronounced, with higher values in upper and bottom ice and lower values in the interior ice layers, and the lowest median bulk salinities were observed. Sea-ice salinity was substantially lower than the mean of seawater values (34.3) throughout the sea-ice cycle, and we observed no clear spatial patterns in sea-ice salinity across the dataset.

3.3. Observed variation in fast-ice macronutrient concentrations

3.3.1. First-year ice

Fig. 3 shows the seasonal variation (monthly median values and interquartile ranges) in measured nutrient concentrations in the upper, interior and bottom ice layers of first-year Antarctic fast ice over the annual cycle. Chlorophyll *a* concentration data from the AFIAC dataset (Meiners et al., 2018) are also shown for each ice layer for comparison to the nutrient data. Fig. 4 shows the vertical distributions of salinity and nutrient concentrations by season sampled. Multi-year sea ice sampled in January and February showed differences compared to first-year ice, so these data are plotted and analysed separately (Fig. 5). Fast-ice nutrient concentrations are compared to concentrations measured in ice-covered or adjacent surface waters, shown in Fig. 6 and presented in Section 3.6. Time series of all fast-ice nutrient concentrations and salinity measurements included in this study are shown in the Supplementary Information (Fig. S1). In first-year ice, a strong seasonal cycle in vertical nutrient distributions was observed from autumn and early winter as the ice was forming through to spring and summer when the ice was melting, decaying and breaking up (Figs. 3, 4). Chlorophyll *a* data show that ice algal biomass was highest in bottom ice over the full seasonal cycle, with large peaks in December and May, which were matched by increases in upper and interior ice albeit to a lesser degree (Fig. 3i).

Nitrate was highest on average in autumn and winter (monthly median up to 6.71 μmol L^{-1} in upper ice in July and 7.54 μmol L^{-1} in bottom ice in June), although values were consistently lower than the underlying surface waters (29.0 ± 1.5 μmol L^{-1}; Fig. 6a) throughout the ice column (Fig. 3c, 4b). Nitrate exhibited a characteristic C-shaped profile, following the salinity profiles, with lowest concentrations in the interior ice layers and gradual increases towards the bottom and upper ice layers. In early spring in October, nitrate was drawn down further in the interior ice layers and some profiles showed increased concentrations above surface water values in the bottom ice layers (Fig. S1a). A small number of cores showed these increases continuing in November, when nitrate concentrations in bottom ice layers at times reached >50 μmol L^{-1}. These high nitrate values close to the ice-water interface occurred in the Ross Sea, East Antarctica and the WAP. Nitrate concentrations throughout the ice column were reduced substantially through December and into mid-summer, except for an increase in bottom ice in January.

Ammonium concentrations were relatively low in general over winter with values similar to surface water values (1.2 ± 0.7 μmol L^{-1}; Fig. 6b) over the full ice profile (Fig. 4c). Median ammonium values were highest in spring, but showed significant variability over this period (Fig. 3d). Ammonium decreased in the interior ice layers from June to October and in bottom ice from June to September; however, in October, ammonium increased in bottom ice layers to values of between 2.5 and 15 μmol L^{-1}. The highest ammonium concentrations were measured in a small number of cores in November ($n = 13$), with maxima of >60 μmol L^{-1} (range 65 to 128 μmol L^{-1}) in the 40–60% and 75–95% depth horizons, which also coincided with maxima in phosphate concentrations (Fig. S1c, d). The high ammonium values in interior and bottom ice layers occurred primarily in the Ross Sea sector (163–173°E). Ammonium concentrations then decreased over the full ice depth through December and into mid-summer to values similar to, or lower than, typical seawater values.

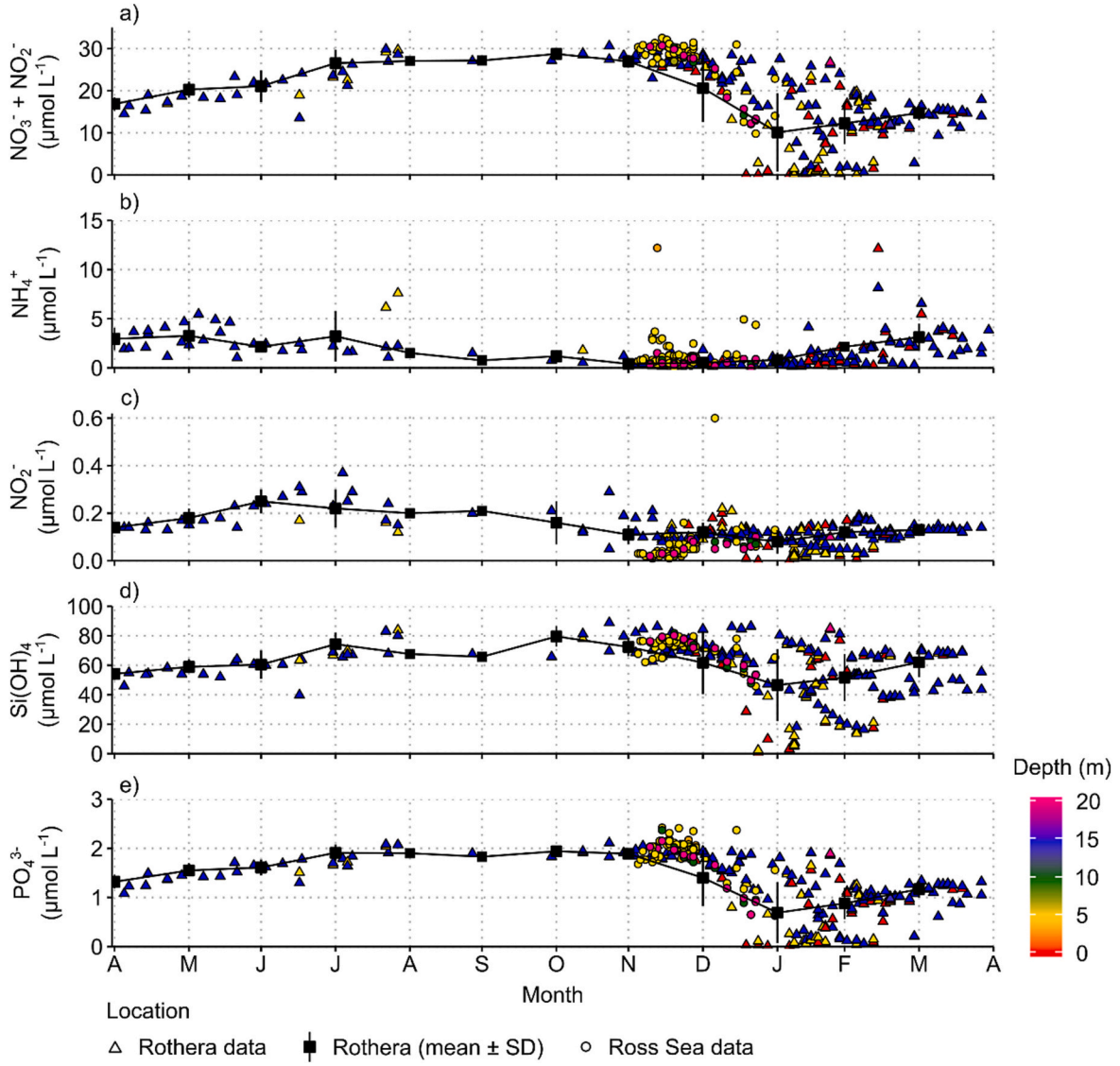

Fig. 6. Seawater nutrient concentrations for the upper 20 m from Marguerite Bay and the eastern Ross Sea: (a) nitrate, (b) ammonium, (c) nitrite, (d) silicic acid, (e) phosphate. Data points are colour-coded by depth, as per legend. Symbol type depicts location and data type: triangles = Rothera data (2013–2016); squares and solid black line = Rothera monthly mean ± SD; circles = Ross Sea data (1997, 1999, 2004). Rothera data are from Henley et al., 2020; Ross Sea data from Cozzi, 2014. Summary data for Marguerite Bay are provided in Table 3 and summary data for the Ross Sea are provided in Table 4.

Nitrite concentrations were consistently low (<0.2 µmol L^{-1}) and similar to surface water values (0.1 ± 0.06 µmol L^{-1}; Fig. 6c), with little variation throughout the ice column in the majority of cores (Fig. 3e, 4d). Slight increases were observed in November with nitrite concentrations reaching 0.25 µmol L^{-1} throughout the ice column and up to 0.45 µmol L^{-1} in bottom ice layers. Extreme values over 0.90 µmol L^{-1} were measured in a small number of cores ($n = 5$). Nitrite concentrations exhibited a C-shaped profile in January with some of the lowest values observed in interior ice and some of the highest concentrations in upper and bottom ice layers.

Total dissolved inorganic nitrogen (nitrate + nitrite + ammonium = DIN) showed a seasonal cycle that reflected that of nitrate and ammonium (Fig. 3f). Substantial accumulation of DIN was observed in bottom ice layers in October and November, and in November concentrations in upper and interior ice also reached their seasonal maxima. DIN concentrations decreased in all ice depth horizons through December and January with the greatest reductions shown in bottom ice layers.

Phosphate exhibited C-shaped profiles in most of the autumn and winter cores, with values lower than surface waters (2.05 ± 0.12 µmol L^{-1}; Fig. 6e) in the interior layers and up to surface water values in bottom and upper ice layers (Fig. 3h, 4f). However, a significant minority of cores showed an accumulation of phosphate in interior ice layers to concentrations higher than surface water values (up to 8 µmol L^{-1}; Fig. S1d). In early spring in October, phosphate concentrations were reduced over most of the ice depth horizons, although phosphate accumulation to values higher than seawater values was observed in some bottom ice layers. These trends continued in November with phosphate concentrations in bottom ice layers reaching >20 µmol L^{-1} in a small number of cores from the Ross Sea. Substantial accumulation was also observed in interior ice layers in a small number of Ross Sea cores, with phosphate concentrations reaching >20 µmol L^{-1} in the 40–60% and 75–90% depth horizons, which corresponded to the ammonium maxima (Fig. S1d, c). Phosphate concentrations decreased substantially in the interior ice from early December and were low (generally <1.5 µmol L^{-1}) for the rest of the month, with less extreme bottom ice values (up to ~5 µmol L^{-1}) and only a small number of cores having increased concentrations in upper ice layers. Phosphate remained low or continued to decrease over all ice depth horizons into mid-summer.

Silicic acid concentrations in sea ice were generally lower than or equal to their corresponding seawater values for most of the seasonal

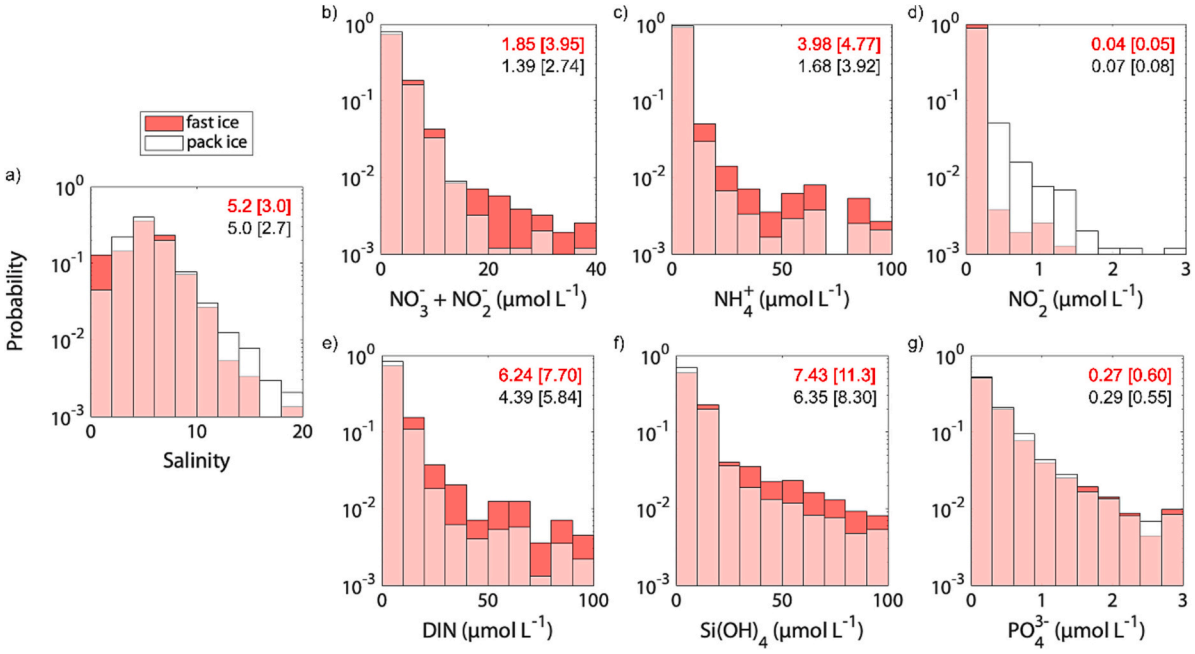

Fig. 7. Frequency histograms of measured (a) salinity and concentrations of (b) nitrate, (c) ammonium, (d) nitrite, (e) DIN, (f) silicic acid and (g) phosphate in fast ice (red, this study) and pack ice (white, Fripiat et al., 2017). Values given are medians and interquartile ranges (in square brackets) for each ice environment (red text = fast ice; black text = pack ice). (For interpretation of the references to colour in this figure legend, the reader is referred to the web version of this article.)

cycle (Fig. 3g, 4e). Concentrations were highest during autumn and winter, and relatively uniform in the majority of cores, although a small number of cores showed high values in bottom ice layers (reaching >150 µmol L^{-1}; Fig. S1b). From winter concentrations that were close to or lower than concurrent seawater values (77.4 ± 2.1 µmol L^{-1}; Fig. 6d), silicic acid was drawn down over the full ice thickness through spring to minimum values in summer (<15 µmol L^{-1}). Silicic acid maxima were observed in bottom ice layers in a small number of cores through October to December, with some correspondence with the high nitrate concentrations in these layers. Our dataset showed no clear spatial patterns in silicic acid concentrations around Antarctica.

3.3.2. *Multi-year ice*

Multi-year fast ice sampled at Syowa Station, Drescher Inlet and in the Ross Sea in January and February showed nutrient and salinity characteristics that were distinct from those of first-year ice and so are considered separately in this analysis (Fig. 5). Neither salinity nor nutrient profiles showed the characteristic C-shape of first-year ice. Salinity values were lower in the majority of multi-year ice cores (<6) than in first-year ice, with minimum values in the upper 25% of the ice thickness (Fig. 5a). The majority of cores showed an overall, yet not monotonic, increase in salinity with ice depth to maximum values in the lower and bottom ice layers. A minority of cores ($n = 3$) showed higher values in the uppermost ice and then rapid declines to minimum values around the 10% depth horizon. A small number of cores (n = 3) showed rapid down-core increases in the upper quarter of the ice thickness to maximum values in the upper 25–50%, before decreasing again to varying degrees over the remaining ice thickness. One core from Drescher Inlet showed a strong increase in bottom ice to a maximum salinity value >10 at the ice-water interface.

Nitrate concentration was low and relatively constant over the full ice thickness in most multi-year ice cores (Fig. 5b). Maximum nitrate concentrations were observed in bottom ice in Drescher Inlet and over the full ice thickness, albeit with relatively large variability, in a core taken at Syowa Station in mid-February. Ammonium concentrations were also low with little variability with ice depth in the majority of cores, although accumulation to >2 µmol L^{-1} was measured in some cores from Syowa Station (Fig. 5c). The highest ammonium values, which were higher than those observed in first-year ice cores at this time of year, were measured in the bottom ice at Drescher Inlet. Nitrite concentrations were generally low and similar to those measured in first-year ice, with some evidence of accumulation in the lower interior ice and bottom ice layers (Fig. 5d). Silicic acid concentrations were also low and similar to first-year ice summer values in the majority of these multi-year fast-ice cores (Fig. 5e). The clear exception to this was the maximum value in bottom ice in Drescher Inlet just above the ice-water interface (44.20 µmol L^{-1}), whilst the value at the ice-water interface was much lower (8.14 µmol L^{-1}), showing fine-scale variability. Phosphate concentrations in multi-year ice were similar to those measured in most first-year ice cores, with the lowest values in the upper quarter of the ice thickness and overall increases with ice depth (Fig. 5f). The highest value (3.00 µmol L^{-1}) was observed at the ice-water interface in Drescher Inlet.

3.4. *Comparison of nutrient concentrations in fast ice and pack ice*

To examine the differences in nutrient concentrations between fast ice and pack ice, we compared frequency histograms based on the fast-ice nutrient data from this compilation and a similar compilation of nutrient data from Antarctic pack ice (Fripiat et al., 2017; Fig. 7). This comparison shows that whilst salinity is indistinguishable between the two ice types (Fig. 7a), concentrations of both nitrate and ammonium, and therefore DIN, are higher and more variable in fast ice (Fig. 7b, c, e). In contrast, nitrite concentration is higher in pack ice (Fig. 7d). Like DIN, silicic acid concentrations are also higher and more variable in fast ice (Fig. 7f), whilst phosphate concentrations are indistinguishable between fast ice and pack ice (Fig. 7g).

3.5. *Nutrient concentrations in platelet ice*

Nutrient concentrations of platelet ice and interstitial water sampled in Drescher Inlet from January to March 1997 and 1998, and in the eastern Ross Sea in November and December 1997, 1999 and 2004 are compared here to those of the overlying fast ice (Table 2; Fig. 8).

Table 2
Nutrient concentrations in sub-ice platelet layer ice, comprising ice platelets (Platelets) and interstitial waters (IW), bottom ice and surface waters (SW) from Drescher Inlet and along the Victoria Land coast, eastern Ross Sea. Time-series data are shown in Fig. 8.

	Platelets+IW (μmol L^{-1})	IW (μmol L^{-1})	Platelets (μmol L^{-1})	Bottom ice (μmol L^{-1})	SW (μmol L^{-1})
Drescher Inlet					
$NO_3^- + NO_2^-$	13.77 ± 2.24	14.20 ± 11.06	8.88 ± 1.19	9.35	
NO_2^-	0.11 ± 0.02	0.12 ± 0.10	0.08 ± 0.03	0.21	
NH_4^+	2.68 ± 1.32	2.51 ± 3.01	3.01 ± 3.50	15.60	
PO_4^{3-}	1.36 ± 0.08	1.31 ± 1.02	2.20 ± 1.16	3.00	
$Si(OH)_4$	24.93 ± 8.65	29.92 ± 24.51	11.95 ± 1.34	8.14–44.20	
Eastern Ross Sea					
NO_3^-	38.56 ± 27.23	24.34 ± 9.50	46.98 ± 23.68	16.19 ± 20.57	27.04 ± 4.98
NO_2^-	0.14 ± 0.08	0.07 ± 0.06	0.24 ± 0.33	0.09 ± 0.09	0.06 ± 0.06
NH_4^+	4.70 ± 4.22	4.40 ± 6.01	9.22 ± 8.34	12.01 ± 12.60	1.00 ± 1.42
PO_4^{3-}	4.39 ± 2.63	2.64 ± 1.79	7.97 ± 8.00	5.46 ± 12.70	1.87 ± 0.38
$Si(OH)_4$	47.55 ± 11.39	60.91 ± 21.93	31.94 ± 13.86	10.82 ± 7.64	72.40 ± 7.66

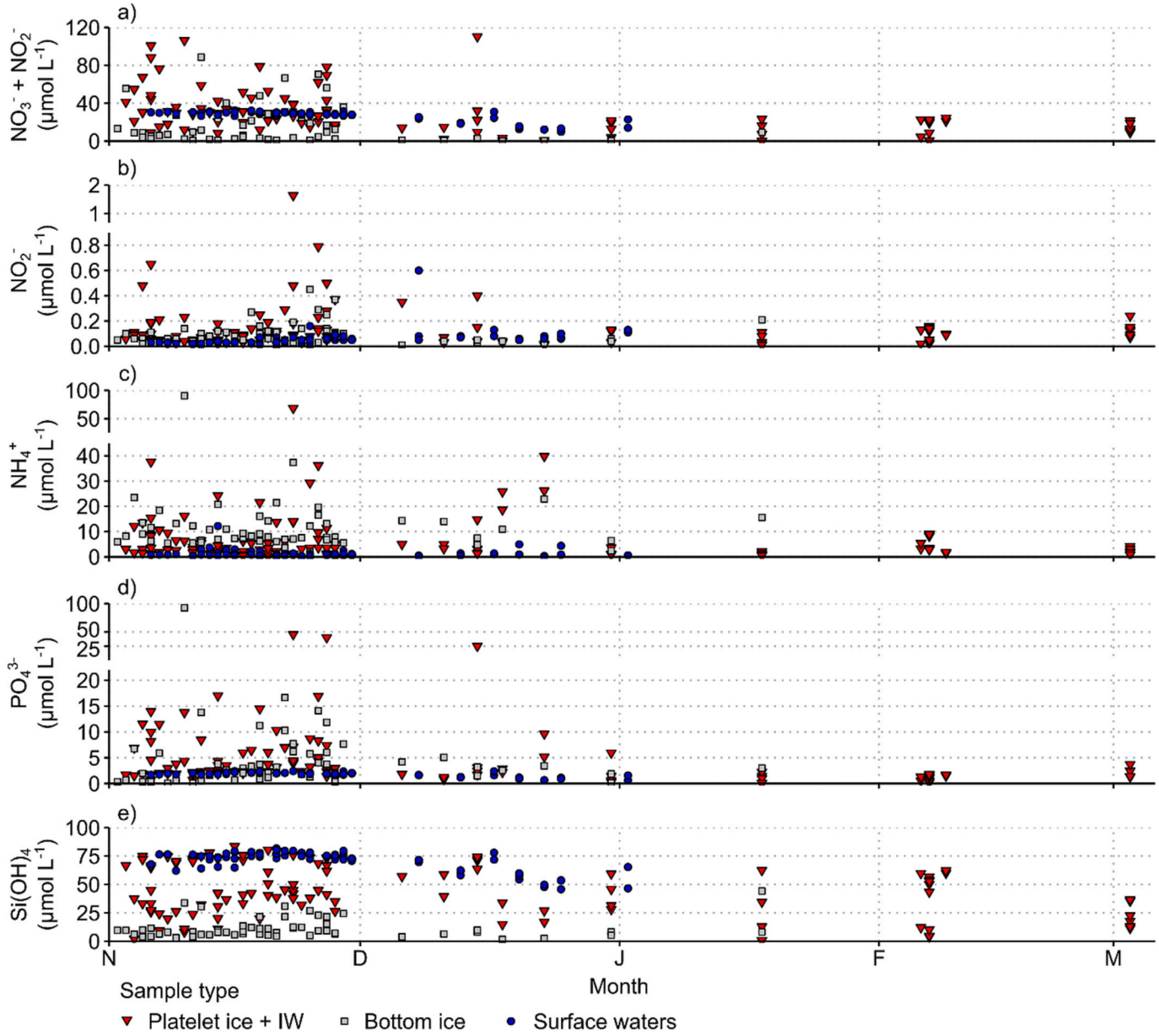

Fig. 8. Time-series plots of concentrations of (a) nitrate, (b) nitrite, (c) ammonium, (d) phosphate and (e) silicic acid in platelet ice and interstitial waters (red triangles), the overlying bottom ice (grey squares) and underlying surface waters (blue circles). Note y-axis breaks in (b)-(d). Data are from the eastern Ross Sea for November (1997, 1999, 2004) and December (2004), and from Drescher Inlet (Weddell Sea) for January and March 1997 and February 1998. Data from each location are summarised in Table 2. (For interpretation of the references to colour in this figure legend, the reader is referred to the web version of this article.)

Underlying surface waters were also sampled in the eastern Ross Sea, so are further compared to platelet ice and interstitial waters.

In Drescher Inlet (January to March), mixed platelet ice and interstitial water showed higher nitrate concentrations than in the overlying ice core bottom layers. Individually, interstitial waters showed higher mean concentrations with large variability, whilst platelets showed concentrations indistinguishable from bottom ice values. Phosphate concentrations in interstitial water and mixed platelet ice and interstitial water were lower than in corresponding bottom ice, whilst the platelets themselves showed concentrations indistinguishable from bottom ice, like nitrate. Silicic acid concentration showed a similar pattern to nitrate, being highly variable in interstitial waters, less variable in mixed platelet ice and interstitial water, and lower and less variable in isolated platelets. Comparison with corresponding bottom ice samples is difficult for silicic acid due to strong variation in the bottom-most ice core sections. Ammonium concentrations in platelet ice and interstitial waters were variable, but substantially lower than in the overlying bottom ice layers. Nitrite concentrations in platelet ice and interstitial waters were also lower than bottom ice values.

For the eastern Ross Sea data (November and December), nutrient concentrations in platelet ice and interstitial water were substantially more variable than those in Drescher Inlet and reached significantly higher values (Table 2; Fig. 8). Platelet ice and interstitial waters both showed concentrations frequently much higher than corresponding seawater values for nitrate, ammonium, nitrite and phosphate. In contrast, silicic acid concentrations in platelet ice and interstitial waters were similar to, or lower than, corresponding seawater values. Compared to concentrations in bottom ice, nitrate and silicic acid concentrations were both significantly higher in platelet ice and interstitial water, with the difference being most pronounced for silicic acid (Fig. 8e). Nitrate concentrations were more similar in November and higher in platelet ice and interstitial waters in December when bottom ice concentrations had declined significantly (Fig. 8a). In contrast, ammonium concentrations were higher overall in bottom ice than in platelet ice and interstitial waters, particularly in November (Fig. 8c). Nitrite and phosphate both showed similar mean concentrations in bottom ice and platelet ice and interstitial waters, with substantial variability over the time series (Fig. 8b, d).

3.6. Nutrient concentrations in surface waters

Surface water (≤20 m) nutrient concentrations from a coastal site in Marguerite Bay over a three-year period (2013 to 2016; Henley et al., 2020) are used to represent the seasonal cycle in locations influenced by fast ice around Antarctica (Fig. 6). These year-round data are compared to seasonal data from the eastern Ross Sea in November 1997 and 1999 and November and December 2004 (Cozzi, 2014). Seasonal minimum and maximum values for Marguerite Bay are shown in Table 3 and monthly values for the eastern Ross Sea are shown in Table 4. Table S2 summarises water column (0–800 m) nutrient concentrations from studies associated with fast ice around Antarctica. Similarity of values and trends across these datasets shows that seasonal variability is substantially larger than spatial variability around Antarctica, such that the Marguerite Bay data presented here are broadly representative of these shelf environments for the purposes of comparing this variability to that in fast ice.

Table 3
Summary data for surface water nutrient concentrations from Marguerite Bay (2013 to 2016) showing seasonal minimum and maximum values (monthly mean ± SD) and their timing. Time-series data are shown in Fig. 6.

	Seasonal minimum		Seasonal maximum	
	Timing (month)	Mean ± SD (μmol L^{-1})	Timing (month)	Mean ± SD (μmol L^{-1})
$NO_3^- + NO_2^-$	January	10.1 ± 9.3	October	28.7 ± 1.2
PO_4^{3-}	January	0.7 ± 0.6	October	1.9 ± 0.1
$Si(OH)_4$	January	46.6 ± 24.3	October	79.6 ± 6.9
NH_4^+	November	0.4 ± 0.3	May	3.3 ± 1.5
NO_2^-	January	0.08 ± 0.05	June	0.25 ± 0.05

Table 4
Summary data for surface water nutrient concentrations from the eastern Ross Sea (1997, 1999, 2004) showing monthly mean values (± SD) for November and December. Time-series data are shown in Fig. 6.

	November mean ± SD (μmol L^{-1})	December mean ± SD (μmol L^{-1})
$NO_3^- + NO_2^-$	28.9 ± 1.4	18.1 ± 6.0
PO_4^{3-}	2.0 ± 0.1	1.2 ± 0.5
$Si(OH)_4$	75.0 ± 3.4	59.9 ± 9.8
NH_4^+	1.0 ± 1.4	1.0 ± 1.4
NO_2^-	0.04 ± 0.02	0.11 ± 0.13

Nitrate, phosphate and silicic acid showed a seasonal cycle characterised by drawdown by spring and summer phytoplankton blooms and subsequent resupply, primarily by vertical mixing, during autumn and winter (Fig. 6a, d, e). Minimum concentrations of each of these nutrients were measured in January and maximum concentrations were reached in October prior to the onset of the phytoplankton bloom (Table 3). Ammonium showed a different seasonal cycle, with minimum values in November and maximum values in May (Fig. 6b). Nitrite reached its seasonal maximum earlier than nitrate in June and its seasonal minimum occurred concurrently with nitrate in January (Fig. 6c).

Seawater nutrient data from the eastern Ross Sea are broadly similar to those from Marguerite Bay, with concentrations of nitrate, phosphate and silicic acid being comparable to seasonal maximum values in Marguerite Bay in November and decreasing in December due to biological drawdown (Fig. 6a, d, e; Table 4). Ammonium values were more variable in the Ross Sea than in Marguerite Bay in November and December, whilst nitrite values were lower in November and similar to those in Marguerite Bay in December (Fig. 6b, c; Table 4).

As sea ice was forming through April, May and June, seawater nitrate, nitrite, phosphate and silicic acid concentrations in Marguerite Bay increased towards their high winter values. Depending on the timing of sea-ice formation, which varies spatially and interannually, concurrent seawater nitrate concentrations ranged from 16.9 ± 1.6 μmol L^{-1} to 21.1 ± 3.7 μmol L^{-1} and nitrite concentrations ranged from 0.14 ± 0.01 μmol L^{-1} to 0.25 ± 0.05 μmol L^{-1} (Fig. 6a, c). Seawater phosphate concentrations during sea-ice formation ranged from 1.3 ± 0.1 μmol L^{-1} to 1.6 ± 0.2 μmol L^{-1}, and silicic acid concentrations ranged from 54.2 ± 4.1 μmol L^{-1} to 60.4 ± 9.7 μmol L^{-1} (Fig. 6d, e). Sea-ice formation coincided with maximum monthly mean ammonium concentrations in surface waters, ranging from 2.1 ± 0.4 μmol L^{-1} to 3.3 ± 1.5 μmol L^{-1} (Fig. 6b).

4. Discussion

4.1. Nutrient supply, uptake and cycling processes in Antarctic fast ice

The major processes affecting nutrient concentrations in Antarctic fast ice are exchange with the underlying surface waters, biological uptake by ice algal communities and remineralisation of organic material, as well as nutrient adsorption to sea-ice surfaces and metal-organic matter complexes, the formation of biofilms and precipitation of minerals (Fripiat et al., 2017; Meiners and Michel, 2017; Roukaerts et al., 2021). These biogeochemical processes are mediated by physical changes in sea-ice characteristics associated with ice formation, melting and break-up. In turn, these physical processes are regulated largely by atmospheric conditions (Fig. 2), in particular, the seasonal cycle of temperature and the mechanical break-up of ice in spring/summer, and also sporadically during winter, due to strong winds from the continent as well as the westerlies and their effect on sea storms and large waves that break the ice. Through these mechanisms, these atmospheric

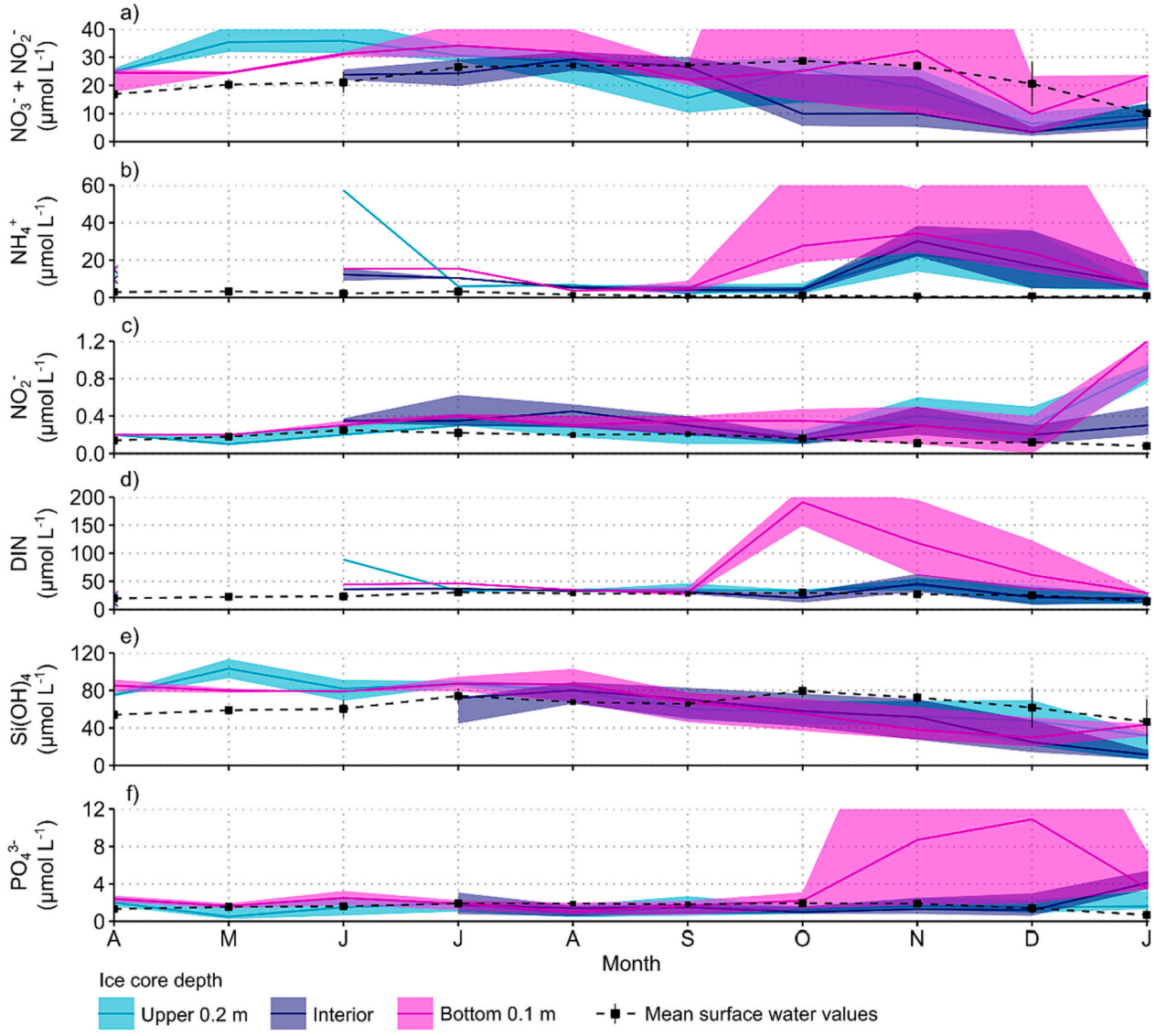

Fig. 9. Time series of salinity-normalised nutrient concentrations in first-year fast ice, (a) nitrate, (b) ammonium, (c) nitrite, (d) DIN, (e) silicic acid, and (f) phosphate. Data are binned by calendar month and shown by ice core depth (where light blue = upper 0.2 m, dark blue = interior, magenta = bottom 0.1 m), with lines connecting monthly median values and shaded areas showing interquartile ranges. x symbols are used in (b) and (d) to indicate monthly median values where no value is available for the previous or following month, with colours indicating core depth. Black squares and dashed lines depict monthly-mean surface water nutrient concentrations ± SD (from Fig. 6), for comparison. Monthly median values for February and March are excluded due to only one fast-ice profile being available for each month. Where monthly data are missing compared to Figs. 3 and 4, this is because bulk sea-ice salinity data were not available to perform the normalisation. (For interpretation of the references to colour in this figure legend, the reader is referred to the web version of this article.)

conditions have an important influence on sea-ice biogeochemistry. Here we use the seasonal patterns in nutrient concentrations and physical parameters described, as well as nutrient stoichiometry and relationships between nutrient concentrations and salinity to examine the major processes governing sea-ice nutrient biogeochemistry and evaluate their importance.

The primary use of nutrients in sea ice is fuelling ice algal primary production, which constitutes a small but ecologically important contribution to biogeochemical cycles in Southern Ocean coastal and marginal ice zones, by providing an early season food source for pelagic and benthic food webs (e.g., Arrigo, 2017). Whilst primary production in the offshore Southern Ocean is generally limited by iron and other essential micronutrients, this study focuses on the macronutrients that are also essential for primary production by ice algal communities and coastal phytoplankton growth. Total ice algal biomass has been shown to be greater in fast ice than in pack ice around Antarctica, and this has been hypothesised to be a consequence of higher availability of both light and nutrients to fast-ice communities (Meiners et al., 2018). Light and nutrient availability are both influenced strongly by the thickness and structure of the ice and overlying snow cover, as well as ice temperature and salinity and their combined effect on ice porosity and permeability (Castellani et al., 2020; Cozzi, 2008). Comparing our dataset with a compilation of Antarctic pack-ice nutrient data (Fripiat et al., 2017) shows that the concentrations of nitrate, ammonium and silicic acid are higher and more variable in fast ice than in pack ice around Antarctica, especially in bottom ice layers (Fig. 7). These findings are consistent with several studies that have shown high nutrient accumulation in coastal sea ice (e.g., Arrigo et al., 1995; Fripiat et al., 2015; Lannuzel et al., 2014; Roukaerts et al., 2021). Higher DIN is likely a result of more intense remineralisation and nutrient retention in fast-ice brine channels (e.g., Fripiat et al., 2015). Higher silicic acid may also be driven partly by this phenomenon, although the higher concentrations in coastal surface waters than the open Southern Ocean are likely to be a more important factor driving the differences between sea-ice

environments. Combined with greater light penetration through a thinner snow cover on fast ice to reach ice algal communities, the higher nutrient availability shown here could sustain higher algal biomass generally observed in fast ice than in pack ice (Meiners et al., 2012, 2018). Higher biomass could also cause the higher DIN and silicic acid concentrations in fast ice by providing more material to be remineralised to inorganic nutrients.

4.2. Nutrient sources and exchange with surface waters

4.2.1. Water masses and surface waters

The total macronutrient inventory in Antarctic sea ice is ultimately controlled by nutrient supply from the underlying seawater; by incorporation of dissolved nutrients as the ice forms from freezing seawater, by incorporation and subsequent remineralisation of organic matter, and by exchange with seawater once the ice has formed through convective processes associated with desalination, tidal pumping and potentially surface flooding (Gleitz and Thomas, 1993; Gleitz et al., 1995; Meiners and Michel, 2017; Vancoppenolle et al., 2010). C-shaped salinity and nutrient profiles reflect the combination of these phenomena and occur primarily due to faster ice growth in the autumn and early winter when ice was thinner, leading to less brine rejection and desalination and, therefore, higher nutrient concentrations in upper ice layers. Slower ice growth later in winter and thus greater brine drainage, desalination and nutrient loss leads to lower salinity and nutrient concentrations in interior ice, and this effect is enhanced by warmer temperatures than in upper ice layers. Increased concentrations in bottom ice are the result of direct convective exchange from surface waters and remineralisation of organic matter accumulated at or close to the ice-water interface, both of which are facilitated by warmer temperatures in the bottom layers than in interior or upper ice (Cozzi, 2014).

In this analysis, we show that the salinity-normalised concentrations of nitrate, phosphate and silicic acid in fast ice are within the range of values measured in coastal surface waters during autumn ice formation (Figs. 6 and 9; Table S2) and maintain a similar range of values to surface waters over winter until August/September. This suggests that spatial and interannual variability in surface water nutrient concentrations as ice forms (Fig. 6; Table S2) is likely to lead to differences in the sea-ice nutrient inventory prior to any ice algal bloom. Surface water nutrient concentrations in autumn/winter are influenced by vertical mixing with deeper nutrient-rich water masses (e.g., circumpolar deep water, high salinity shelf water), which is enhanced by seasonally strong winds (Fig. 2d), as well as the degree of biological nutrient uptake by phytoplankton blooms in the preceding summer growing season and subsequent remineralisation of the organic matter produced (Henley et al., 2020; Henley et al., 2017). Whilst the coastal regions where fast ice is found receive a greater supply of iron than the open Southern Ocean (Dinniman et al., 2020), such that biological nutrient uptake is greater, macronutrient drawdown to limiting concentrations is rare in Antarctic surface waters (Henley et al., 2020; Moreau et al., 2019). The timing of sea-ice formation during autumn and winter when nutrient replenishment by enhanced vertical mixing is already underway also contributes to surface water nutrient concentrations being consistently high enough to provide a nutrient source to sea ice (e.g., Gibson and Trull, 1999; Gleitz and Thomas, 1993). This nutrient source is likely to be larger for fast ice in the Antarctic than the Arctic, where deep winter mixing is less efficient and surface water nutrient concentrations are significantly lower and can limit primary production during the summer growing season (Mills et al., 2018; Reigstad et al., 2002; Tremblay et al., 2015). The higher productivity of Antarctic coastal surface waters than further offshore during summer also facilitates entrainment of some particulate and detrital organic matter into the sea ice as it forms in autumn, sometimes leading to phytoplankton and ice algal blooms (e.g., Lieser et al., 2015). Evidence for such autumn blooms is seen in fast-ice chlorophyll *a* data, with the largest biomass accumulations in the bottom layers close to the ice-water interface (Fig. 3i; Meiners et al., 2018). These blooms then undergo subsequent remineralisation to provide an additional source of nutrients within the ice matrix, at times elevating concentrations above surface water values (Janssens et al., 2016).

4.2.2. Platelet ice and enhanced nutrient supply

The formation of sub-ice platelet layers and their subsequent consolidation into incorporated platelet ice results in convection which can also promote nutrient inputs to sea ice from surface waters in regions close to or downstream of ice shelves (Günther and Dieckmann, 1999). Our findings of nutrient concentrations in sub-ice platelet layers in the Ross and Weddell Seas being higher on average than in surrounding surface waters for nitrate, nitrite, ammonium and phosphate suggest that the initial supply of seawater nutrients is supplemented by remineralisation of organic matter that was both scavenged from the water column as the platelet layer formed and produced in situ, in agreement with previous work (Arrigo et al., 1995; Dieckmann et al., 1992; Günther and Dieckmann, 1999). In particular, the observation of higher nitrite in the platelet layer indicates higher rates of bacterial nitrification than in surface waters (Arrigo et al., 1995; see Section 4.3.3). Silicic acid concentrations being lower in platelet ice and interstitial waters than in surface waters is consistent with slower rates of diatom frustule dissolution compared to organic matter remineralisation, such that biological uptake of silicic acid by diatoms exceeds its regeneration in the platelet layer (Günther and Dieckmann, 1999). Higher nitrate and silicic acid in the platelet layer than the overlying bottom ice is likely to reflect biological uptake by high algal standing stocks including diatoms in bottom ice. This gradient in nitrate and silicic acid concentrations would then promote their supply from the platelet layer to the bottom ice by diffusive processes. Lower concentrations on average of ammonium, nitrite and phosphate in the platelet layer than bottom ice implicate more intense remineralisation of a larger algal biomass in the semi-closed bottom ice matrix. Overall, our data show that nutrient accumulation within the platelet layer and subsequent incorporation into the ice matrix can enhance the supply of seawater nutrients into fast ice around Antarctica and support previous assertions that this process is likely to be more effective for fast-ice platelet layers than pack ice (Arrigo et al., 1995).

4.2.3. Tidal currents and enhanced nutrient supply

Under-ice tidal currents have been shown to enhance nutrient supply to sea ice by increasing brine convection and promoting exchange with surface waters (Cota et al., 1987; Eicken, 1992; Vancoppenolle et al., 2013). The strength of these currents is influenced in turn by water depth, bottom topography, and proximity to glaciers and ice shelves (Sun et al., 2019). A recent study has shown elevated turbulence in the ocean surface boundary layer under fast ice in Marguerite Bay (compared to ice-free conditions), which could also promote the supply of nutrients to the sea ice from surface waters (Inall et al., 2022). As fast ice is present over shallower waters than pack ice, tidal currents are expected to be stronger under fast ice than pack ice (Richter et al., 2022), further leading to greater ice-ocean exchanges of dissolved and particulate constituents. These stronger tidal currents could thus contribute to explaining greater nutrient supply and potentially higher ice algal biomass in fast ice (see Section 4.1), as has been observed in East Antarctica (Roukaerts et al., 2021) as well as the Canadian Arctic (Dalman et al., 2019; Mortenson et al., 2017).

4.2.4. Sedimentary nutrient supply

Sedimentary nutrient fluxes to the water column can also influence ice-ocean nutrient exchanges when sea ice occurs near the sedimentary source or downstream in waters that are influenced by sedimentary fluxes from which nutrients are subsequently transferred to sea ice (de Jong et al., 2013; DeMaster et al., 1996). Sedimentary silicic acid fluxes have been shown to be significant in the WAP shelf region, driven by diatom frustule dissolution and reverse weathering reactions (Cassarino et al., 2020), and are likely to be the most important sedimentary

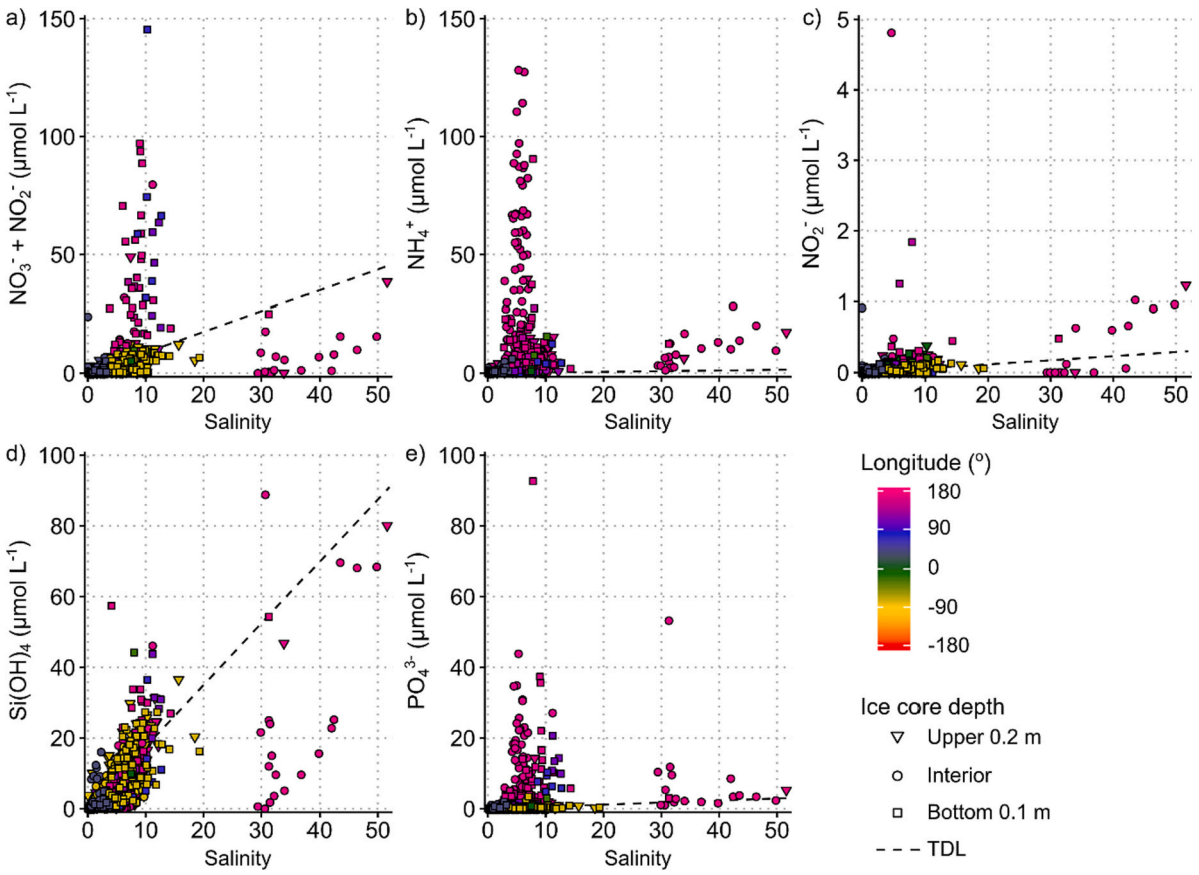

Fig. 10. Nutrient-salinity plots for all ice types showing (a) nitrate, (b) ammonium, (c) nitrite, (d) silicic acid, (e) phosphate. Data points are colour-coded by longitude as per legend and the symbols depict ice core depth (triangle = upper 0.2 m, circle = interior, square = bottom 0.1 m). Dashed black lines are theoretical dilution lines (TDLs) depicting conservative relationships of each nutrient with salinity.

macronutrient flux influencing sea-ice biogeochemistry in coastal Antarctica. Sedimentary denitrification has been measured in Antarctic shelf settings (Hartnett et al., 2008) and could cause a water column nitrogen deficit over shallow continental shelves, as has been observed in the Arctic (Chang and Devol, 2009; Fripiat et al., 2018). Table S2 shows such a nitrogen deficit, compared to the Redfield ratio of 16N:1P, in some shallow coastal areas around Antarctica where fast ice is known to occur, indicating that sedimentary denitrification could influence nutrient content in the ice. However, in general Antarctic shelves are much deeper than their Arctic counterparts, such that the effect of sedimentary denitrification on Antarctic fast ice is expected to be small overall. Sediment-derived nutrients may also be transferred directly to the ice matrix along continental margins where sea ice is attached to the coast, although this effect is likely to be highly localised and not a major nutrient supply mechanism for Antarctic fast ice more widely.

4.2.5. *Surface flooding and snow cover*

Snow cover on top of sea ice can facilitate nutrient delivery to the sea-ice matrix from surface waters by depressing the ice-snow interface below the sea surface and causing surface water flooding of the snow and upper ice layers (Tison et al., 2017). Subsequent formation of snow ice, under the weight of overlying snow as the flooded snow/slush layer freezes, can incorporate seawater nutrients into the ice matrix (Maksym and Jeffries, 2000; Sturm and Massom, 2009, 2017). In our dataset, approximately half of the ice cores are accompanied by measurements of snow thickness ($n = 128$), of which most had snow cover of less than 0.5 m and only five had a ratio of snow thickness to ice thickness of >1:3 indicating flooding. Amongst the small number of cores that have freeboard measurements ($n = 11$), a negative freeboard required for surface flooding was only observed in one first-year ice core from the Dronning Maud Land coast. Although there was little evidence for surface flooding at the time of sampling across our dataset, C-shaped salinity and nutrient profiles may be indicative of surface flooding having occurred over the ice-covered period, particularly for profiles that were or had been close to the ice edge or cracks and leads in the ice cover. Seawater inflow to the upper ice layers would have become possible through spring as increasing air temperatures (Fig. 2b) warmed the upper ice, producing a more permeable matrix than during winter when these layers were cold and impermeable. These effects of surface flooding would be superimposed onto the seasonal evolution of salinity and nutrient profiles driven by variability in brine drainage and convection with depth and time (Cozzi, 2014) and biological processes (Sections 4.3.2, 4.3.3).

Snow can also act as a reservoir for nutrients that are supplied by atmospheric deposition or from land (Nowak et al., 2018) and can subsequently percolate into the sea-ice brine network, as suggested in the case of iron (Duprat et al., 2019; Lannuzel et al., 2016a), or be incorporated into the ice matrix through the formation of snow ice or superimposed ice. Superimposed ice is formed from snow alone when accumulation is insufficient to depress the ice-snow interface below the sea surface, such that meltwater from the shallowest snow permeates the interface below the freezing point and refreezes (Kawamura et al., 1997; Nomura et al., 2018). Superimposed ice formation can be important for supplying micronutrients such as iron (Lannuzel et al., 2016a), but its effect on macronutrients is more likely to be one of dilution rather than enrichment. This has been shown recently near Syowa Station, where high rates of snow fall and accumulation (Toyota et al., 2016) lead to the formation of both snow ice and superimposed ice (Kawamura et al., 1997; Nomura et al., 2018; Nomura et al., 2012). Superimposed ice is low in nutrients due to low concentrations in snow on top of the sea ice

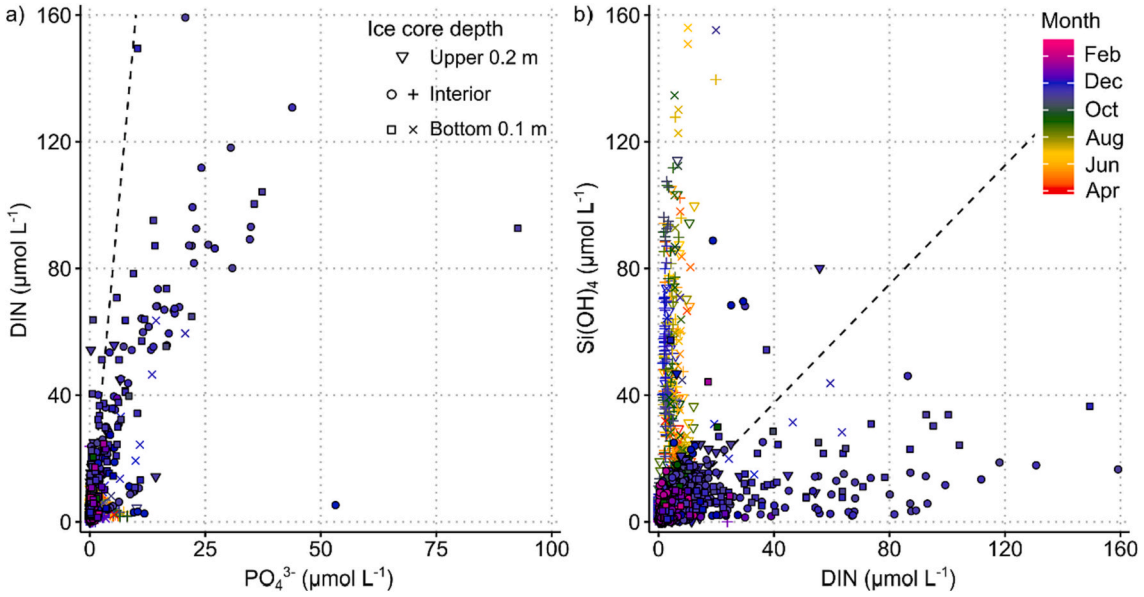

Fig. 11. Nutrient-nutrient plots showing measurements from all ice types: (a) DIN-phosphate; (b) silicic acid-DIN. Filled symbols depict when ammonium data were available and show DIN concentrations; open symbols depict when ammonium data were not available to calculate DIN, so nitrate concentrations are plotted instead. Symbols depict ice core depth: triangles = upper 0.2 m, circles and crosses = interior, squares and x symbols = bottom 0.1 m. Data points are colour-coded by sampling date from 1 April (red) to mid-February (magenta) each year, according to the legend. Both legends apply to both plots. Dashed black lines show the expected relationships based on the Redfield N:P ratio and the 1:1 Si:N ratio expected for nutrient uptake by iron-replete diatoms. (For interpretation of the references to colour in this figure legend, the reader is referred to the web version of this article.)

(Sahashi et al., 2022); a consequence of Antarctica's distance from areas of human activity and resultant purity of the air, compared to that in the Northern Hemisphere. Our data show that multi-year ice has a much thicker snow cover (0.56 ± 0.42 m) than first-year ice (0.13 ± 0.07 m) in this region, such that these dilution effects are likely to be more pronounced in multi-year ice, which dominates over first-year ice around Syowa Station (Fraser et al., 2021). Our multi-year ice data (Fig. 5) show that macronutrient concentrations are lower in the upper ice horizons than in interior and bottom ice and decrease in the upper ice over time due to replacement by clean snow each year. This is fully consistent with superimposed ice formation diluting nutrient concentrations in upper ice layers, with this effect being particularly pronounced for multi-year ice (Sahashi et al., 2022).

Of the mechanisms of nutrient supply to Antarctic fast ice described here, we conclude that platelet ice accumulation and under-ice tidal currents are important in enhancing convective and diffusive nutrient fluxes, with a more minor role for surface flooding. The rate and extent of nutrient exchange between the ice matrix and the underlying seawater is influenced strongly by ice temperature, salinity, and the thickness and structure of the ice and overlying snow. As a result of the underlying seawater being the major source for Antarctic fast-ice nutrients, it is the nutrient concentrations of those surface waters – as regulated by water masses, mixing, sedimentary nutrient supply and biological processes – that ultimately control the total nutrient inventory of sea ice.

4.3. Seasonal nutrient dynamics and major processes

4.3.1. Influence of physical and biogeochemical processes on seasonal nutrient cycles

Changes in sea-ice nutrient concentrations in space, time and with ice depth are driven by a combination of biological, biogeochemical and physical processes influencing nutrients directly and indirectly. Here we use plots of bulk nutrient concentrations as a function of salinity (Fig. 10) alongside time series of salinity-normalised nutrient concentrations (Fig. 9) to elucidate the most important processes at work over the seasonal cycle around Antarctica. A conservative relationship of bulk nutrient concentrations with salinity shows that changes in nutrient concentrations are driven by concentration or dilution during sea-ice freezing and melting (i.e., physical processes), and is indicated by a theoretical dilution line (TDL) constructed as a linear regression from wintertime surface water values (Fig. 10). Departures from the TDL indicate nutrient depletion or enrichment by biological processes. Spatial and temporal changes in salinity-normalised nutrient concentrations (Fig. 9) reveal further the importance of biological and biogeochemical processes in sea ice that are independent of physical changes in sea-ice properties. We also examine the relationships between DIN, phosphate and silicic acid, in comparison to those expected from biological nutrient uptake and remineralisation stoichiometry, as characterised by the Redfield ratio of 16:1 for N:P and the 1:1 ratio of Si:N expected for iron-replete pelagic diatoms (Fig. 11). This enables us to explore the coupling and decoupling of nitrogen, phosphorus and silicon cycles in Antarctic fast ice over the seasonal cycle (Section 4.3.3).

Seasonal cycles of salinity-normalised nitrate, phosphate and silicic acid concentrations in sea ice provide evidence for nutrient supply from surface waters and biological uptake by ice algal communities (Fig. 9). Salinity-normalised nitrate, phosphate and silicic acid concentrations that are within the observed range of surface water values (Table S2) in autumn and winter, with most bulk values plotting along or close to the TDL (Fig. 10), show that nutrients are supplied to the sea-ice matrix from underlying seawater as the ice forms and by subsequent ice-ocean exchanges. Consistent trends in sea ice and the underlying surface waters (Fig. 6) show further that the effects of enhanced vertical mixing of the water column in autumn and winter on upper ocean nutrient concentrations are also reflected in sea-ice nutrient inventories.

4.3.2. Biological nutrient drawdown linked to ice algal production

Biological drawdown of nitrate, phosphate and silicic acid is shown from early spring (September) to mid-summer (December/January) by overall reductions in salinity-normalised concentrations (Fig. 9). Superimposed onto these trends are accumulations of nitrate and phosphate in October and November in some bottom ice layers where biomass is accumulating rapidly (see Section 4.3.3). The overall reductions show some correspondence with decreasing salinity from

November to January, indicating a contribution to these trends from nutrient (and salinity) loss by enhanced brine drainage as seasonal-maximum air temperatures (Fig. 2b) lead to ice warming, melting and increased permeability. However, bulk concentrations plotting below their respective TDLs in nutrient-salinity space (Fig. 10) confirm that these seasonal declines are driven primarily by biological uptake by ice algal communities. This is consistent with seasonal chlorophyll *a* data (Fig. 3i), which show that ice algal biomass increases rapidly in bottom ice layers, and to a lesser extent in upper and interior ice, from September as the sun returns to high southern latitudes, increasing PAR (Fig. 2c) and initiating biomass accumulation (Meiners et al., 2018). The summertime peak in chlorophyll *a* concentrations in all ice layers in December (Fig. 3i) coincides with seasonal minima of nitrate in all ice layers and silicic acid in bottom ice (Fig. 9a, e). The timing of minimum monthly median values and maximum month-to-month drawdown does vary amongst the three nutrients and between ice horizons, because of differences in uptake stoichiometry, which are probably related to variations in ice algal community composition with ice depth and time. There is some evidence for more intense nutrient drawdown in interior ice and slightly higher concentrations in upper and bottom ice, leading to more pronounced C-shaped profiles than observed in winter and early spring, especially for nitrate. We attribute these changes to nutrient drawdown being offset to a degree in bottom and upper ice by replenishment from surface waters, potentially including surface flooding, and remineralisation (Section 4.3.3) during the growing season.

Sustained drawdown of silicic acid over the entire period of biomass accumulation and overall nitrate and phosphate drawdown implicates diatoms as major contributors to the ice algal community. Biological uptake acts as a dominant process impacting silicon dynamics in fast ice and draws down silicic acid to concentrations similar to or lower than those observed in underlying or adjacent shelf surface waters (Fig. 6; Table S2). Coincidence of the minimum monthly silicic acid concentration with the nitrate minimum and the chlorophyll *a* maximum in bottom ice implies a diatom-dominated ice algal community where biomass is highest (van Leeuwe et al., 2022). In contrast, minimum silicic acid concentrations were reached a month later than minimum nitrate concentrations in the upper and interior ice layers and the most rapid monthly decrease in silicic acid occurred two months later than that of nitrate in interior ice. This suggests that there was a significant contribution to primary production and nutrient uptake in upper and interior ice by non-siliceous flagellates (in addition to diatoms), such as the haptophyte *Phaeocystis* sp., as has been observed in a range of Southern Ocean settings and in the Arctic (Arrigo et al., 2014; Becquevort et al., 2009; Torstensson et al., 2015; van Leeuwe et al., 2018). This vertical structure in community composition is reinforced by the molar $Si(OH)_4$:NO_3^-, $Si(OH)_4$:DIN and $Si(OH)_4$:PO_4^{3-} ratios all being lower in bottom ice where diatoms dominate than in interior or upper ice layers, and gradually decreasing from early spring into summer (Fig. S2). Further, the relative timing of the most pronounced drawdown periods of silicic acid (November to December) and nitrate (September to October) in interior and upper ice suggests a succession in the algal community from a mixed assemblage including flagellates in the early part of the productive period to a greater dominance of diatoms approximately two months later (Jones et al., 2022; van Leeuwe et al., 2018; van Leeuwe et al., 2022). This is also supported by the temporal trends of the molar $Si(OH)_4$:NO_3^-, $Si(OH)_4$:DIN and $Si(OH)_4$:PO_4^{3-} ratios that all show increases in interior ice for October (Fig. S2) when we infer that flagellates were more prevalent in the ice algal assemblage, and subsequent declines as diatoms become more abundant.

4.3.3. Nutrient regeneration and recycling within the ice matrix

Substantial accumulations of DIN and phosphate superimposed onto overall trends of biological drawdown during spring and summer are observed in several fast-ice cores. Salinity-normalised concentrations in excess of surface water values (Fig. 9) and bulk values plotting above the TDLs (Fig. 10) indicate biological enrichment of these nutrients by organic matter remineralisation and nutrient recycling within the ice matrix. Our dataset shows significantly higher salinity-normalised ammonium concentrations in sea ice than surface water values for most of the seasonal cycle in all ice layers and bulk values plot consistently above the TDL. The largest ammonium accumulations occur in bottom ice in October and November, and in interior ice in November, particularly in the Ross Sea and adjacent to the Adélie Land coast. We also observed a significant accumulation of nitrate in bottom ice in some cores in October and November, with bulk values (>20 μmol L^{-1}) plotting significantly above the TDL, particularly in the Ross Sea and around East Antarctica. Combined with seasonal trends in salinity-normalised DIN, these observations of the individual inorganic nitrogen forms provide strong evidence for intense biological nitrogen recycling within the sea-ice matrix, particularly in the spring and early summer (Arrigo et al., 1995; Cozzi, 2008; Cozzi, 2014; Fripiat et al., 2015). This occurs coincident with substantial accumulation of algal biomass (Fig. 3i; Meiners et al., 2018) and shows that primary production and organic matter remineralisation can occur simultaneously within the ice matrix, likely in microenvironments, e.g., biofilms, with distinct biogeochemical dynamics (Roukaerts et al., 2021; Section 4.5). Uptake by the ice algal community of ammonium as an alternative nitrogen source to nitrate becomes more important as the growing season proceeds (Kristiansen et al., 1998) and has been shown to make a larger contribution to primary production in the interior ice than in bottom ice close to the ice-water interface (Roukaerts et al., 2016). Such uptake of ammonium as well as nitrate is likely to influence concentrations of both inorganic nitrogen forms in our dataset (Priscu and Sullivan, 1998; Thomas and Dieckmann, 2002).

Nitrification plays a key role in nitrogen recycling and provides a critical regenerative pathway back to nitrate, as evidenced in winter by increases in salinity-normalised nitrite concentration in all ice layers between May and August and in spring/summer by substantial accumulations of nitrate in some bottom ice in October and November and elevated nitrite values in all ice layers in January. This is consistent with ammonium oxidising bacteria being found in Antarctic sea-ice assemblages (Priscu et al., 1990) and shows that nitrification can occur when light limitation is sufficient to allow nitrifiers to outcompete ice algae for the available ammonium (Fripiat et al., 2014a; Fripiat et al., 2015). Such light limitation is expected in winter when insolation is at or close to its seasonal minimum (Fig. 2), but can also occur in spring and summer when ice and/or the overlying snow are thick enough for light attenuation to lead to limiting conditions in the bottom ice or through the ice column (Castellani et al., 2020; Fripiat et al., 2015). It is also plausible that in distinct microenvironments within the ice matrix (Roukaerts et al., 2021; Section 4.5), ice algae are limited by a factor other than light availability during spring and summer, such as silicic acid availability for diatom-dominated communities (Section 4.4). Nevertheless, we propose that light limitation linked to ice and potentially snow thickness is the primary control on spring/summer nitrification in our dataset, because this is observed most readily in January when all ice sampled was thicker than 1.4 m (Fig. 3).

Phosphate also shows significant accumulation above surface water values in bottom ice through November and December, as well as in interior ice in January and in the same cores from the Ross Sea and adjacent to the Adélie Land coast from November that showed large peaks in ammonium concentration. This biological enrichment of phosphate concurrent with that of inorganic nitrogen provides further evidence for intense organic matter remineralisation. Such accumulations of phosphate, ammonium and nitrate well above surface water values strongly suggest efficient nutrient pumping into the ice matrix, high levels of accumulation into biomass and subsequent high rates of heterotrophic activity by bacterial communities and grazers coupled with substantial nitrogen and phosphorus recycling (e.g., Arrigo et al., 1995; Günther et al., 1999; Roukaerts et al., 2021; Thomas et al., 1998). There is also evidence for accumulation of ammonium and phosphate, as well as dissolved organic matter, in interior ice that had clearly been

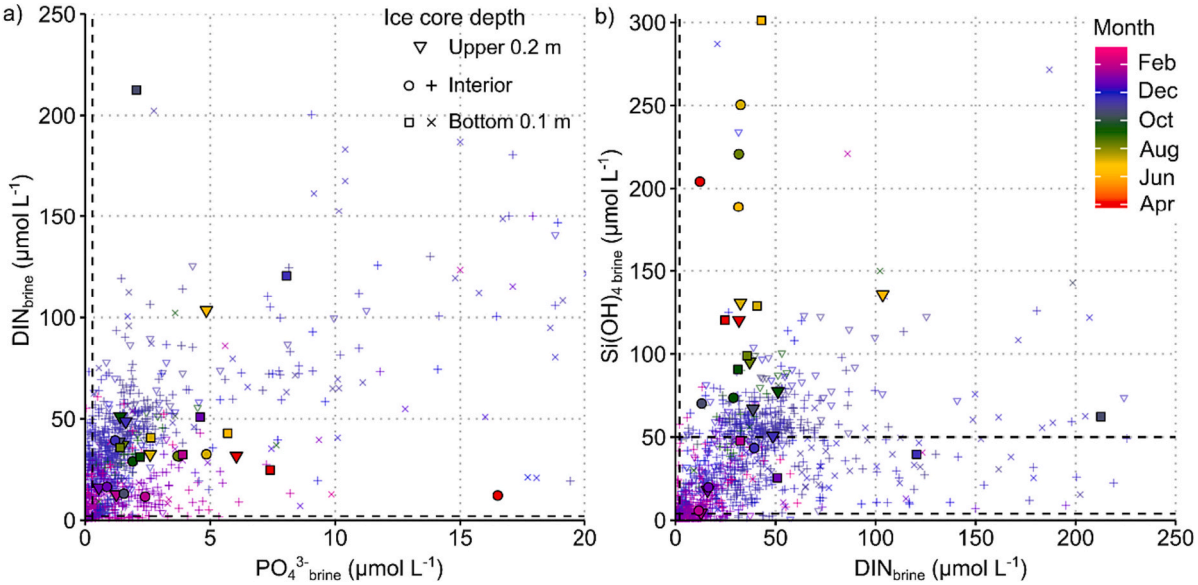

Fig. 12. Nutrient-nutrient plots showing estimated individual (smaller open symbols) and monthly median (larger filled symbols) concentrations in fast ice brine from all ice types: (a) DIN-phosphate; (b) silicic acid-DIN. Symbols are colour-coded by sampling date from 1 April (red) to mid-February (magenta) each year, according to the legend. Ice core depth is represented by symbol type as follows: triangles = upper 0.2 m, circles and crosses = interior, squares and x symbols = bottom 0.1 m. Dashed black lines show representative concentrations below which nutrient limitation is known to occur (DIN = 2 µmol L^{-1}; phosphate = 0.3 µmol L^{-1}), and measured and estimated values for the nutrient half-saturation constant for silicic acid (K_{Si} = 3.9 µmol L^{-1} and 50 µmol L^{-1}; see text for more details). (For interpretation of the references to colour in this figure legend, the reader is referred to the web version of this article.)

impacted by a previous break-out event and refreezing, such that nutrient accumulation can also be driven by decay of organic detritus entrapped episodically in the ice as well as remineralisation of algal biomass produced in situ (Cozzi, 2014).

We found no statistically significant difference in phosphate concentrations between fast ice and pack ice (Fig. 7; median values of 0.27 and 0.29 µmol L^{-1}, respectively), suggesting that phosphate accumulation due to organic matter remineralisation and nutrient recycling occurs to a comparable degree between these ice environments around Antarctica. Similar to observations of pack ice (Fripiat et al., 2017), our dataset shows that phosphate accumulation in fast ice is greater than that of nitrate and/or ammonium, according to the Redfield ratio of 16N:1P (Fig. 11a), which leads to a reduction in the molar N:P ratio through spring and early summer (Fig. S2). This strongly suggests that in addition to organic matter remineralisation producing both phosphate and inorganic nitrogen, there must also be preferential assimilation and remineralisation of phosphorus relative to nitrogen. This would be consistent with greater resource allocation by ice algae to phosphorus-rich ribosomes (growth machinery) during rapid growth (Arrigo, 2005; Klausmeier et al., 2004), coupled with convective loss of excess DIN, and/or organic phosphorus being more labile and thus having a shorter turnover time than organic nitrogen (Clark et al., 1998; Letscher and Moore, 2015; Loh and Bauer, 2000). The degree of phosphate accumulation in excess of DIN accumulation shown here cannot be accounted for by these uptake and remineralisation effects alone, so there must be additional processes occurring that produce excess phosphate without producing DIN. Phosphate adsorption onto metal-organic matter complexes (Fripiat et al., 2017; Maranger and Pullin, 2003; Yuan and Lavkulich, 1994; Zhou et al., 1997) could be facilitated by high concentrations of decaying organic matter and trace metals in sea ice (e.g., Becquevort et al., 2009; Dumont et al., 2009; Lannuzel et al., 2011; Thomas et al., 2001), and phosphate release may also occur during dissolution of abiotic calcium carbonate (ikaite; $CaCO_3.6H_2O$) (see Section 4.6).

Dissolution of diatom frustules alongside organic matter remineralisation can be an important component of silicon cycling in sea ice and is strongly influenced by bacterial activity (Bidle and Azam, 1999), grazing (Thomas and Dieckmann, 2002), frustule surface area and composition, and environmental conditions such as temperature, salinity and pH (Barker et al., 1994; Greenwood et al., 2001; Martin-Jézéquel et al., 2000). Silicic acid polymerisation may also play a significant role in regulating the availability of silicon and dissolution of biogenic silica, yet these intricate processes are often neglected in sea ice. Given that polymerisation is known to be sensitive to temperature, pH, saturation and salinity (Chan, 1989), we could expect it to be important in sea ice brine channels with low temperatures, high salinities and varying pH, particularly in portions of the ice with high rates of diatom growth, death and dissolution, and therefore high silicic acid concentrations. Polymerisation may be less important closer to the ice-water interface in the open brine network where conditions are less extreme, but further work is required to better constrain its influence across sea-ice environments.

Here, the large accumulations of DIN and phosphate during spring/early summer are not accompanied by accumulations of silicic acid to the degree expected according to the 1:1 $Si(OH)_4$:DIN ratio for nutrient uptake by iron-replete diatoms and subsequent remineralisation, and instead plot below this ratio (Fig. 11b). This suggests that organic matter remineralisation occurs faster, over shorter timescales, and to a greater extent than diatom frustule dissolution (Dugdale et al., 1995) and may also reflect the contributions to nutrient uptake and subsequent recycling of non-siliceous species in addition to diatoms. These processes also contribute to gradual decreases in the $Si(OH)_4$:DIN and $Si(OH)_4$:PO_4^{3-} ratios in all ice layers over spring and early summer, as silicic acid is primarily being drawn down whilst phosphate and DIN are also accumulating due to organic matter remineralisation. Nevertheless, we do observe significant increases in silicic acid concentrations and $Si(OH)_4$:DIN and $Si(OH)_4$:PO_4^{3-} ratios in bottom ice in January, which provide evidence for some degree of diatom frustule dissolution. Consistent with findings from Antarctic pack ice (Fripiat et al., 2017), this shows that diatom frustule dissolution occurs to a greater extent in sea ice than in the underlying surface waters (Fripiat et al., 2014b; Henley et al., 2018). This difference is most likely a consequence of the relatively slow rates of biogenic silica dissolution (e.g., specific dissolution rates of 0.01 to 0.19 d^{-1}; Nelson et al., 1991), such that the longer

residence times of diatoms in sea ice allow greater dissolution than in the surface ocean, despite the lower temperatures.

4.4. Nutrient limitation of sea-ice algae

Low sea-ice nutrient concentrations, particularly during mid-summer in upper and interior ice layers, may limit primary production by sympagic algae (Arrigo and Thomas, 2004; Vancoppenolle et al., 2013). Primary producers become nutrient-limited when the concentration of one or more nutrients is insufficient to sustain maximum growth rates. Light and nutrient co-limitation are also common in this environment as a result of the high latitude and seasonal cycle of insolation and PAR (Fig. 2c) and the attenuation of light by sea ice and the overlying snow cover (Castellani et al., 2020; Maykut and Untersteiner, 1971). Whilst iron is often the limiting nutrient in Antarctic surface waters, this is unlikely to be the case in fast ice, where concentrations of iron are significantly higher than both pack ice and surface seawaters (Lannuzel et al., 2016b). In contrast, complete exhaustion of inorganic nitrogen, phosphate and silicic acid has been documented and shown to have significant effects on ice algal biochemistry (Gleitz et al., 1996; Gleitz and Thomas, 1993; Lizotte and Sullivan, 1992; McMinn et al., 1999). To assess the potential for nutrient limitation across our Antarctic fast ice dataset, we estimate the concentration of DIN, phosphate and silicic acid available to sympagic organisms in sea-ice brine, following Fripiat et al. (2017). Measurements of sea-ice temperature were not available for most ice cores in our dataset, therefore brine nutrient concentrations could not be estimated using brine volume fractions (Cox and Weeks, 1983). Instead, we approximate brine volume fraction as the maximum expected ice porosity typical of warm and saline Antarctic sea ice, 20% (e.g., Tison et al., 2008). Individual measured values for DIN, phosphate and silicic acid and monthly median values for each in upper, interior and bottom ice layers were divided by this porosity (0.2) to estimate brine nutrient concentrations, which were then compared to measured or estimated values for nutrient half-saturation constants or concentrations below which nutrient limitation is known to occur.

Nutrient-nutrient plots of these estimated brine values (Fig. 12) compare the degree of limitation between DIN and phosphate, and silicic acid and DIN. The representative threshold DIN concentration is given as 2 μmol L^{-1} based on an upper bound for phytoplankton in the euphotic zone (Moore et al., 2013), whilst that of phosphate (0.3 μmol L^{-1}) is given as an upper bound based on the lowest brine concentration estimated using this method for Antarctic pack ice and the median value measured in sack-hole brines in spring-summer (Fripiat et al., 2017). These representative thresholds are not based on half-saturation constants for nutrient uptake measured for ice algae, but they are taken to be reasonable estimates based on available literature. Whilst none of the monthly median values for DIN or phosphate fall below these representative thresholds, suggesting that neither nitrogen- nor phosphorus-limitation are prevalent in the fast ice that we observed, our analysis does indicate sporadic limitation by one or both nutrients in several individual data points plotting below these thresholds (Fig. 12a). These limiting conditions are most common in interior ice during late spring and summer (November to February), concurrent with or following the increase in ice algal biomass from September to December (Fig. 3; Meiners et al., 2018). Phosphate reaches limiting conditions more frequently than DIN, and in upper and occasionally bottom ice, as well as the interior layers. Accumulation of phosphate and DIN concurrent with algal biomass in some bottom ice sections during spring/summer prevents them reaching limiting conditions despite substantial uptake, because these nutrients are resupplied to the algal community by organic matter remineralisation during the growth period (Section 4.3.3).

Limitation of sea-ice diatoms by silicic acid availability has been inferred in fast ice at Davis Station, East Antarctica, when silicic acid concentrations were mostly below 12 μmol L^{-1} (Lim et al., 2019). Similarly low silicic acid concentrations (<10 μmol L^{-1}) in surface waters in the Ross Sea ice-edge zone during summer have also been found to limit diatom growth (Nelson and Tréguer, 1992). Lim et al. (2019) also showed that the affinity of fast-ice diatoms for silicic acid may be substantially lower than pelagic diatoms, building on previous work that showed a decreased affinity at low temperatures (Stapleford and Smith, 1996). Lim et al. (2019) used a one-dimensional physical-biogeochemical sea ice model to show that observed chlorophyll *a* and silicic acid concentrations were best explained by a half-saturation constant for silicic acid uptake (K_{Si}) of 50 μmol L^{-1}. This is substantially higher than the K_{Si} of 3.9 μmol L^{-1} that has been measured for cultured pelagic diatoms (Sarthou et al., 2005), which is consistent with observational results from Ross Sea surface waters showing K_{Si} values of 1.1 to 4.6 μmol L^{-1} (Nelson and Tréguer, 1992). Whilst similarly high K_{Si} values have been measured in pelagic diatoms south of the Polar Front in the Pacific Sector of the Southern Ocean, surface water values are generally much lower (Nelson et al., 2001). The much higher value for K_{Si} in fast ice (Lim et al., 2019) is supported by unpublished experimental results from C. W. Sullivan (referenced in Arrigo et al., 1993) and previous modelling work (Arrigo and Sullivan, 1994; Saenz and Arrigo, 2012; Saenz and Arrigo, 2014). Fig. 12b shows that using the representative value for pelagic diatoms (3.9 μmol L^{-1}; Sarthou et al., 2005) would indicate that silicon limitation is not prevalent in our dataset, and only occurs sporadically during the summer, similar to nitrogen- and phosphorus-limitation. However, a higher value of K_{Si}, as indicated by Lim et al. (2019), would mean that diatoms could experience silicon limitation in all ice layers in summer, with the most intense limitation occurring in upper and interior ice in January (and December) and in bottom ice in December. A plausible explanation for higher K_{Si} would be the typically larger cell sizes of sea-ice diatoms, thus greater demand for silicic acid, which could also have implications for DIN and phosphate demand, as well as micronutrients. We recommend future studies, including targeted laboratory experiments, that aim to reduce the uncertainty around the affinity of sea-ice diatoms for silicic acid and the affinity of all ice algae for nitrate, ammonium and phosphate, which may also differ significantly from pelagic phytoplankton (Thomas and Dieckmann, 2002). Nevertheless, our data suggest that silicon limitation can be more prevalent in Antarctic fast-ice algae than nitrogen- or phosphorus-limitation, due to stronger biological drawdown and slower recycling rates, and this may exert an important control on ice algal community composition (Section 4.3.2).

4.5. Nutrient adsorption to sea-ice surfaces and the role of biofilms

Accumulations of ammonium, phosphate and nitrate that we observe in spring and summer, to concentrations higher than seawater values (Fig. 9; Section 4.3.3), are consistent with previous studies showing retention of nutrients within the brine network, such that concentrations measured in sack-hole brine were lower than the bulk ice concentrations for ammonium and phosphate (Fripiat et al., 2017), as well as iron (Lannuzel et al., 2016b). Adsorption of nutrients to ice surfaces was put forward as a likely process facilitating such retention, with the presence and high concentrations of decaying organic matter and extracellular polymeric substances (EPS) in sea ice promoting nutrient recycling, adhesion to ice and retention within the brine system (Deming and Collins, 2017; Meiners et al., 2008; Underwood et al., 2010). While possible in the case of ammonium, phosphate and iron, Roukaerts et al. (2021) suggest that the complexation to EPS of other anions including nitrate cannot explain their accumulation in bottom fast ice. This is also supported in Fripiat et al. (2017) where no difference was reported for nitrate between sack-hole and bulk ice concentrations. However, another characteristic of EPS is that they can form a biofilm, where microorganisms aggregate and adhere to surfaces via self-produced EPS, creating a gel-like polymer network (Davey and O'Toole, 2000; Decho, 2000; Kokare et al., 2009). These biofilms retain decaying products (including nutrients) in close proximity to the sympagic community and could explain observations of nutrients (including nitrate) accumulating

during the growth season (Roukaerts et al., 2021). The presence of biofilms has also been hypothesised to be required to explain observations from several short-term time-series studies (Fripiat et al., 2015; Lim et al., 2019; Riaux-Gobin et al., 2013; Thomas and Dieckmann, 2002; van der Merwe et al., 2011) of high nutrient concentrations in association with high chlorophyll *a* (or particulate organic carbon) in bottom fast ice, the so-called nutrient-chlorophyll paradox (Roukaerts et al., 2021). By using a combination of conceptual and NPZD models (with and without biofilms), Roukaerts et al. (2021) showed that the presence of biofilms would best explain field observations from three highly productive sites in East Antarctica and allow both nutrient uptake by autotrophs and production by heterotrophs to occur at the same time and in close proximity to each other. The autotrophs and heterotrophs cohabiting in the biofilm, within a sub-centimetre spatial scale, allow the spatial decoupling between nutrient production and loss terms as well as the co-occurrence of high biomass and high nutrients observed in bottom fast ice.

4.6. Abiotic removal of phosphate

Time series of salinity-normalised nutrient concentrations show that phosphate is drawn down in all ice layers in August, and to the lowest monthly median value observed in bottom ice (Fig. 9). This occurs prior to the return of the sun to high southern latitudes and sufficient increase in PAR to instigate primary production (Fig. 2c), and earlier than the trend of biological drawdown shown by nitrate. This earlier drawdown cannot be explained by photosynthetic uptake and may instead be explained by phosphate co-precipitation with ikaite in the low-temperature, high brine salinity and low-porosity conditions characteristic of Antarctic winter (Dieckmann et al., 2008; Hu et al., 2014; Jones et al., 2022; Moreau et al., 2015; Papadimitriou et al., 2013; Rysgaard et al., 2014). Whilst further work is required to better-define the importance of mineral precipitation and dissolution in coupled biogeochemical cycles, the seasonal patterns shown here emphasise the complexity and diversity of phenomena influencing sea-ice nutrient cycling, including both biotic and abiotic processes.

5. Conclusions and implications

We present a major international compilation of nutrient concentration data from Antarctic fast ice, and describe the key biogeochemical processes cycling nitrogen, phosphorus and silicon within the ice matrix and the exchange of nutrients between fast ice, surface waters and snow cover. Nutrients are supplied to fast ice primarily from underlying surface waters by direct exchange across the ice-water interface. This exchange is driven largely by convective processes associated with desalination, and fluxes are enhanced by higher surface water nutrient concentrations, platelet ice accumulation, and under-ice tidal currents. Comparison of our nutrient dataset with the AFIAC compilation of fast-ice chlorophyll *a* data (Meiners et al., 2018) shows that nutrient uptake by ice algal communities during spring and summer leads to reductions in nutrient concentrations in many cases. Strong drawdown of silicic acid indicates the importance of diatoms in the ice algal assemblage, particularly in bottom ice where biomass is greatest. In other cases, we observed large accumulations of inorganic nitrogen and phosphate in spring and early summer concurrent with substantial biomass accumulation, especially in bottom and interior ice layers. This supports previous work showing that primary production and organic matter remineralisation can occur simultaneously in fast ice (Roukaerts et al., 2021), and shows that the resultant nutrient recycling was particularly intense in these layers. These accumulations may be enhanced by nutrient adsorption to sea-ice surfaces and/or the presence of biofilms. Accumulation of silicic acid occurs later and to a lesser degree due to slower rates of diatom frustule dissolution. We have shown that sporadic limitation of primary production by nitrogen or phosphate can occur in Antarctic fast ice, although limiting conditions for these nutrients are neither widespread nor sustained across our dataset. A lower affinity of sea-ice diatoms than pelagic diatoms for silicic acid, as well as strong drawdown and slower recycling of silicic acid, could mean that silicon limitation is more widespread in fast ice, but further work is required to better-quantify the affinities for all nutrients amongst sea-ice algal communities, which could differ significantly from pelagic phytoplankton.

Overall, we found that concentrations of nitrate, ammonium and silicic acid were all higher in fast ice than in pack ice around Antarctica, and we attribute this difference to greater supply from underlying seawater and more intense recycling of organic matter. We conclude that greater nutrient availability, particularly of silicic acid which is most likely to be limiting, is potentially an important factor in explaining generally more elevated algal biomass in fast ice than pack ice, alongside greater light availability due to thinner snow cover in coastal fast-ice environments (Meiners et al., 2012, 2018). In sum, this study shows that the cycling of nitrogen, phosphorus and silicon in Antarctic fast ice, and their exchange with surface waters, are modulated by a combination of physical and biological processes over the seasonal cycle, with the relative importance of these processes varying in time and space.

Many of the processes involved in nutrient cycling in fast-ice environments are sensitive to ongoing and anticipated climate change. For example, continued warming would likely reduce ice and snow thickness and increase porosity and permeability earlier in the spring season, likely leading to an increase in nutrient supply to the ice matrix through enhanced exchange with the surface ocean. As well as increasing the availability of nutrients to sympagic biological communities, such warming effects on the ice structure would increase the amount of light and habitable space for ice algal growth (Fraser et al., 2023). Resultant changes in the timing, magnitude and duration of ice algal blooms would then alter the uptake and recycling of nutrients within the ice matrix, thus influencing subsequent exchanges with the surface ocean. A more detailed explanation of how future changes in Antarctic fast ice may affect primary production is provided in Fraser et al. (2023).

The most significant impact on fast-ice nutrient cycling at the circumpolar scale will be widespread losses of Antarctic sea ice, such as those that have been observed since 2014 (Eayrs et al., 2021; Fraser et al., 2023; Parkinson, 2019). These unprecedented declines in total Antarctic sea-ice extent – and fast-ice extent specifically – will have reduced the area of the Southern Ocean where fast-ice nutrient cycling has a direct influence on the surface waters and ecosystems associated with the ice. This effect will be especially pronounced along stretches of the Antarctic coastline where fast ice has reduced vastly in area or disappeared completely, as observed during the record-low sea-ice extents in mid-late summer 2022 and 2023 (Fraser et al., 2023; United States National Snow and Ice Data Center, 2023, URL: https://nsidc.org/arcticseaicenews/sea-ice-tools/). However, in the areas where fast ice does persist, the nutrient cycling processes that we have described here are likely to become ever more important in their role in supporting ice algal primary production, providing an important early-season food source for pelagic and benthic food webs, and in exchanging nutrients with the surrounding ocean. These changes in fast-ice coverage and duration are likely to have cascading effects throughout Antarctic marine food webs, including overall reductions in ice algal primary production due to smaller habitat ranges and shorter habitable periods (Fraser et al., 2023), shifts in distributions of species reliant on the early-season food source and habitat provision from fast ice (Swadling et al., 2023), and potential large-scale implications for Southern Ocean biogeochemistry, including nutrient cycling (Henley et al., 2020).

CRediT authorship contribution statement

Sian F. Henley: Conceptualization, Methodology, Validation, Formal analysis, Investigation, Resources, Data curation, Writing – original draft, Visualization, Supervision, Project administration.

Stefano Cozzi: Data curation, Writing – original draft, Writing – review & editing, Visualization. **François Fripiat:** Conceptualization, Methodology, Data curation, Writing – review & editing. **Delphine Lannuzel:** Writing – original draft, Writing – review & editing. **Daiki Nomura:** Writing – original draft, Writing – review & editing. **David N. Thomas:** Writing – original draft, Writing – review & editing. **Klaus M. Meiners:** Writing – review & editing. **Martin Vancoppenolle:** Methodology, Software, Validation, Formal analysis, Resources, Visualization. **Kevin Arrigo:** Writing – review & editing. **Jacqueline Stefels:** Writing – review & editing. **Maria van Leeuwe:** Writing – review & editing. **Sebastien Moreau:** Writing – review & editing. **Elizabeth M. Jones:** Writing – review & editing. **Agneta Fransson:** Writing – review & editing. **Melissa Chierici:** Writing – review & editing. **Bruno Delille:** Writing – review & editing. In addition to the above, all authors contributed to investigation and data curation by providing data for the circumpolar compilation on which this study is based.

Declaration of Competing Interest

The authors declare that there are no conflicts of interest, financial or otherwise, associated with this manuscript.

Data availability

All data used in this study are publicly available or were obtained from published work. Compiled nutrient concentration data from Antarctic fast-ice cores and platelet ice are available through the Australian Antarctic Data Centre (URL: https://data.aad.gov.au/metadata/BEPSII_2023_Fast_Ice_Nutrients). Seawater nutrient concentration data from Rothera Station (2013–2016) are available from the British Oceanographic Data Centre at https://www.bodc.ac.uk/data/published_data_library/catalogue/10.5285/98cc0722-e337-029c-e053-6c86abc02029/ (Henley and Venables, 2019). All other data are published, with references given in the text, tables and/or figure captions.

Henley, S. F., and Venables, H. J. (2019). Water Column Nutrient, Particulate Organic Matter and Isotopic Data for Ryder Bay, West Antarctic Peninsula 2013–2016. Liverpool: British Oceanographic Data Centre, National Oceanography Centre. doi: https://doi.org/10.5285/98cc0722-e337-029c-e053-6c86abc02029.

Acknowledgements

SFH was supported by the United Kingdom Natural Environment Research Council through grant NE/K010034/1. KMM was supported by the Australian Government through Australian Antarctic Science Project #4546, through the Antarctic Science Collaboration Initiative program (project ID ASCI000002), and through the Australian Research Council's Australian Centre for Excellence in Antarctic Science (Project Number SR200100008). These funders had no influence or involvement in the study design, execution or the preparation of the article.

This study was carried out under the auspices of the international expert group on Biogeochemical Exchange Processes at Sea-Ice Interfaces (BEPSII), which was originally a Working Group of the Scientific Committee on Oceanic Research (SCOR; WG-140) and has since been endorsed by the Scientific Committee on Antarctic Research (SCAR), the Surface Ocean Lower Atmosphere Study (SOLAS) and Climate and Cryosphere (CliC). This study was also supported by the Southern Ocean Observing System (SOOS) and the data will be available through SOOS' open-access data portal SOOSmap (https://soos.aq/data/soosmap).

The authors would like to thank the editor and three reviewers for their thorough and careful review and handling of our manuscript, which have undoubtedly improved the final paper.

Appendix A. Supplementary data

Supplementary data to this article can be found online at https://doi.org/10.1016/j.marchem.2023.104324.

References

Abernathey, R.P., Cerovecki, I., Holland, P.R., Newsom, E., Mazloff, M., Talley, L.D., 2016. Water-mass transformation by sea ice in the upper branch of the Southern Ocean overturning. Nat. Geosci. 9 (8), 596–601. https://doi.org/10.1038/ngeo2749.

Ackley, S.F., Sullivan, C.W., 1994. Physical controls on the development and characteristics of Antarctic Sea ice biological communities— a review and synthesis. Deep-Sea Res. I Oceanogr. Res. Pap. 41 (10), 1583–1604. https://doi.org/10.1016/0967-0637(94)90062-0.

Arndt, S., Hoppmann, M., Schmithüsen, H., Fraser, A.D., Nicolaus, M., 2020. Seasonal and interannual variability of landfast sea ice in Atka Bay, Weddell Sea, Antarctica. Cryosphere 14 (9), 2775–2793. https://doi.org/10.5194/tc-14-2775-2020.

Arrigo, K.R., 2005. Marine microorganisms and global nutrient cycles. Nature 437 (7057), 349–355. https://doi.org/10.1038/Nature04158.

Arrigo, K.R., 2014. Sea ice ecosystems. Annu. Rev. Mar. Sci. 6 (6), 439–467. https://doi.org/10.1146/annurev-marine-010213-135103.

Arrigo, K.R., 2017. Sea ice as a habitat for primary producers. In: Thomas, D.N. (Ed.), Sea Ice, 3rd edition. Wiley-Blackwell, Oxford, U. K., pp. 352–369 ISBN: 978-1-118-77838-8.

Arrigo, K.R., Sullivan, C.W., 1994. A high resolution bio-optical model of microalgal growth: tests using sea-ice algal community time-series data. Limnol. Oceanogr. 39 (3), 609–631. https://doi.org/10.4319/lo.1994.39.3.0609.

Arrigo, K.R., Thomas, D.N., 2004. Large scale importance of sea ice biology in the Southern Ocean. Antarct. Sci. 16 (4), 471–486. https://doi.org/10.1017/S0954102004002263.

Arrigo, K.R., Kremer, J.N., Sullivan, C.W., 1993. A simulated Antarctic fast ice ecosystem. J. Geophys. Res. Oceans 98 (C4), 6929–6946. https://doi.org/10.1029/93jc00141.

Arrigo, K.R., Dieckmann, G., Gosselin, M., Robinson, D.H., Fritsen, C.H., Sullivan, C.W., 1995. High-resolution study of the platelet ice ecosystem in Mcmurdo sound, Antarctica - biomass, nutrient, and production profiles within a dense microalgal bloom. Mar. Ecol. Prog. Ser. 127 (1–3), 255–268. https://doi.org/10.3354/Meps127255.

Arrigo, K.R., Robinson, D.H., Dunbar, R.B., Leventer, A.R., Lizotte, M.P., 2003. Physical control of chlorophyll a, POC, and TPN distributions in the pack ice of the Ross Sea, Antarctica. J. Geophys. Res. Oceans 108 (C10). https://doi.org/10.1029/2001jc001138.

Arrigo, K.R., Brown, Z.W., Mills, M.M., 2014. Sea ice algal biomass and physiology in the Amundsen Sea, Antarctica. Elementa: Sci. Anthropocene 2, 000028. https://doi.org/10.12952/journal.elementa.000028.

Barker, P., Fontes, J.-C., Gasse, F., 1994. Experimental dissolution of diatom silica in concentrated salt solutions and implications for paleoenvironmental reconstruction. Limnol. Oceanogr. 39 (1), 99–110. https://doi.org/10.4319/lo.1994.39.1.0099.

Becker, S., Aoyama, M., Woodward, E.M.S., Bakker, K., Coverly, S., Mahaffey, C., Tanhua, T., 2020. GO-SHIP repeat hydrography nutrient manual: the precise and accurate determination of dissolved inorganic nutrients in seawater, using continuous flow analysis methods. Front. Mar. Sci. 7 https://doi.org/10.3389/fmars.2020.581790.

Becquevort, S., Dumont, I., Tison, J.L., Lannuzel, D., Sauvée, M.L., Chou, L., Schoemann, V., 2009. Biogeochemistry and microbial community composition in sea ice and underlying seawater off East Antarctica during early spring. Polar Biol. 32 (6), 879–895. https://doi.org/10.1007/s00300-009-0589-2.

Bidle, K.D., Azam, F., 1999. Accelerated dissolution of diatom silica by marine bacterial assemblages. Nature 397 (6719), 508–512. https://doi.org/10.1038/17351.

Bluhm, B.A., Swadling, K.M., Gradinger, R., 2017. Sea ice as a habitat for macrograzers. In: Thomas, D.N. (Ed.), Sea Ice, 3rd edition. Wiley-Blackwell, Oxford, U. K, pp. 394–414. ISBN: 978-1-118-77838-8.

Caldeira, K., Duffy, P.B., 2000. The role of the Southern Ocean in uptake and storage of anthropogenic carbon dioxide. Science 287 (5453), 620–622. https://doi.org/10.1126/science.287.5453.620.

Cassarino, L., Hendry, K.R., Henley, S.F., MacDonald, E., Arndt, S., Freitas, F.S., Pike, J., Firing, Y.L., 2020. Sedimentary nutrient supply in productive hot spots off the West Antarctic peninsula revealed by silicon isotopes. Glob. Biogeochem. Cycles 34 (12). https://doi.org/10.1029/2019GB006486 e2019GB006486.

Castellani, G., Schaafsma, F.L., Arndt, S., Lange, B.A., Peeken, I., Ehrlich, J., David, C., Ricker, R., Krumpen, T., Hendricks, S., Schwegmann, S., Massicotte, P., Flores, H., 2020. Large-scale variability of physical and Biological Sea-ice properties in polar oceans. Front. Mar. Sci. 7 https://doi.org/10.3389/fmars.2020.00536.

Chan, S.H., 1989. A review on solubility and polymerization of silica. Geothermics 18 (1), 49–56. https://doi.org/10.1016/0375-6505(89)90009-6.

Chang, B.X., Devol, A.H., 2009. Seasonal and spatial patterns of sedimentary denitrification rates in the Chukchi Sea. Deep-Sea Res. II Top. Stud. Oceanogr. 56 (17), 1339–1350. https://doi.org/10.1016/j.dsr2.2008.10.024.

Clark, L.L., Ingall, E.D., Benner, R., 1998. Marine phosphorus is selectively remineralized. Nature 393 (6684). https://doi.org/10.1038/30881, 426–426.

Cota, G.F., Prinsenberg, S.J., Bennett, E.B., Loder, J.W., Lewis, M.R., Anning, J.L., Watson, N.H.F., Harris, L.R., 1987. Nutrient fluxes during extended blooms of Arctic ice algae. J. Geophys. Res. Oceans 92 (C2), 1951–1962. https://doi.org/10.1029/JC092iC02p01951.

Cox, G.F.N., Weeks, W.F., 1983. Equations for determining the gas and brine volumes in sea-ice samples. J. Glaciol. 29 (102), 306–316. https://doi.org/10.3189/S0022143000008364.

Cozzi, S., 2008. High-resolution trends of nutrients, DOM and nitrogen uptake in the annual sea ice at Terra Nova Bay, Ross Sea. Antarct. Sci. 20 (5), 441–454. https://doi.org/10.1017/S0954102008001247.

Cozzi, S., 2014. Multiscale variability of ambient conditions, fast ice dynamics and biogeochemistry in the coastal zone of Victoria land, Ross Sea. Antarct. Sci. 26 (4), 427–444. https://doi.org/10.1017/S0954102013000813.

Cozzi, S., Cantoni, C., 2011. Stable isotope (δ13C and δ15N) composition of particulate organic matter, nutrients and dissolved organic matter during spring ice retreat at Terra Nova Bay. Antarct. Sci. 23 (1), 43–56. https://doi.org/10.1017/S0954102010000611.

Dalman, L.A., Else, B.G.T., Barber, D., Carmack, E., Williams, W.J., Campbell, K., Duke, P.J., Kirillov, S., Mundy, C.J., 2019. Enhanced bottom-ice algal biomass across a tidal strait in the Kitikmeot Sea of the Canadian Arctic. Elementa: Sci. Anthropocene 7, 22. https://doi.org/10.1525/elementa.361.

Davey, M.E., O'Toole, G.A., 2000. Microbial biofilms: from ecology to molecular genetics. Microbiol. Mol. Biol. Rev. 64 (4), 847–867. https://doi.org/10.1128/mmbr.64.4.847-867.2000.

de Jong, J., Schoemann, V., Maricq, N., Mattielli, N., Langhorne, P., Haskell, T., Tison, J.-L., 2013. Iron in land-fast sea ice of McMurdo Sound derived from sediment resuspension and wind-blown dust attributes to primary productivity in the Ross Sea, Antarctica. Mar. Chem. 157, 24–40. https://doi.org/10.1016/j.marchem.2013.07.001.

Decho, A.W., 2000. Microbial biofilms in intertidal systems: an overview. Cont. Shelf Res. 20 (10), 1257–1273. https://doi.org/10.1016/S0278-4343(00)00022-4.

Delille, B., Vancoppenolle, M., Geilfus, N.-X., Tilbrook, B., Lannuzel, D., Schoemann, V., Becquevort, S., Carnat, G., Delille, D., Lancelot, C., Chou, L., Dieckmann, G.S., Tison, J.-L., 2014. Southern Ocean CO2 sink: the contribution of the sea ice. J. Geophys. Res. Oceans 119 (9), 6340–6355. https://doi.org/10.1002/2014JC009941.

DeMaster, D.J., Ragueneau, O., Nittrouer, C.A., 1996. Preservation efficiencies and accumulation rates for biogenic silica and organic C, N, and P in high-latitude sediments: the Ross Sea. J. Geophys. Res. Oceans 101 (C8), 18501–18518. https://doi.org/10.1029/96jc01634.

Deming, J.W., Collins, E.R., 2017. Sea ice as a habitat for bacteria, archaea and viruses. In: Thomas, D.N. (Ed.), Sea Ice, Third edition. Wiley-Blackwell, Oxford, U.K., pp. 326–351. https://doi.org/10.1002/9781118778371.ch13 ISBN: 978-1-118-77838-8.

DeVries, T., 2014. The oceanic anthropogenic CO2 sink: storage, air-sea fluxes, and transports over the industrial era. Glob. Biogeochem. Cycles 28 (7), 631–647. https://doi.org/10.1002/2013gb004739.

Dieckmann, G.S., Arrigo, K., Sullivan, C.W., 1992. A high-resolution sampler for nutrient and chlorophyll a profiles of the sea ice platelet layer and underlying water column below fast ice in polar oceans - preliminary-results. Mar. Ecol. Prog. Ser. 80 (2–3), 291–300. https://doi.org/10.3354/meps080291.

Dieckmann, G.S., Nehrke, G., Papadimitriou, S., Göttlicher, J., Steininger, R., Kennedy, H., Wolf-Gladrow, D., Thomas, D.N., 2008. Calcium carbonate as ikaite crystals in Antarctic Sea ice. Geophys. Res. Lett. 35 (8) https://doi.org/10.1029/2008GL033540.

Dinniman, M.S., St-Laurent, P., Arrigo, K.R., Hofmann, E.E., van Dijken, G.L., 2020. Analysis of iron sources in Antarctic continental shelf waters. J. Geophys. Res. Oceans 125. https://doi.org/10.1029/2019JC015736 e2019JC015736.

Dore, J.E., Houlihan, T., Hebel, D.V., Tien, G., Tupas, L., Karl, D.M., 1996. Freezing as a method of sample preservation for the analysis of dissolved inorganic nutrients in seawater. Mar. Chem. 53 (3), 173–185. https://doi.org/10.1016/0304-4203(96)00004-7.

Dugdale, R.C., Wilkerson, F.P., Minas, H.J., 1995. The role of a silicate pump in driving new production. Deep-Sea Res. Part I-Oceanogr. Res. Pap. 42 (5), 697–719. https://doi.org/10.1016/0967-0637(95)00015-X.

Dumont, I., Schoemann, V., Lannuzel, D., Chou, L., Tison, J.L., Becquevort, S., 2009. Distribution and characterization of dissolved and particulate organic matter in Antarctic pack ice. Polar Biol. 32 (5), 733–750. https://doi.org/10.1007/s00300-008-0577-y.

Duprat, L., Kanna, N., Janssens, J., Roukaerts, A., Deman, F., Townsend, A.T., Meiners, K. M., van der Merwe, P., Lannuzel, D., 2019. Enhanced iron flux to Antarctic Sea ice via dust deposition from ice-free coastal areas. J. Geophys. Res. Oceans 124 (12), 8538–8557. https://doi.org/10.1029/2019JC015221.

Eayrs, C., Li, X., Raphael, M.N., Holland, D.M., 2021. Rapid decline in Antarctic Sea ice in recent years hints at future change. Nat. Geosci. 14 (7), 460–464. https://doi.org/10.1038/s41561-021-00768-3.

Eicken, H., 1992. The role of sea ice in structuring Antarctic ecosystems. Polar Biol. 12 (1), 3–13. https://doi.org/10.1007/BF00239960.

Fawcett, S.E., Lomas, M.W., Ward, B.B., Sigman, D.M., 2014. The counterintuitive effect of summer-to-fall mixed layer deepening on eukaryotic new production in the Sargasso Sea. Glob. Biogeochem. Cycles 28 (2), 86–102. https://doi.org/10.1002/2013gb004579.

Fletcher, S.E.M., Gruber, N., Jacobson, A.R., Doney, S.C., Dutkiewicz, S., Gerber, M., Follows, M., Joos, F., Lindsay, K., Menemenlis, D., Mouchet, A., Muller, S.A., Sarmiento, J.L., 2006. Inverse estimates of anthropogenic CO2 uptake, transport, and storage by the ocean. Glob. Biogeochem. Cycles 20 (2). https://doi.org/10.1029/2005gb002530.

Fransson, A., Chierici, M., Yager, P.L., Smith Jr., W.O., 2011. Antarctic Sea ice carbon dioxide system and controls. J. Geophys. Res. Oceans 116 (C12). https://doi.org/10.1029/2010JC006844.

Fraser, A.D., Massom, R.A., Ohshima, K.I., Willmes, S., Kappes, P.J., Cartwright, J., Porter-Smith, R., 2020. High-resolution mapping of circum-Antarctic landfast sea ice distribution, 2000–2018. Earth Syst. Sci. Data 12 (4), 2987–2999. https://doi.org/10.5194/essd-12-2987-2020.

Fraser, A.D., Massom, R.A., Handcock, M.S., Reid, P., Ohshima, K.I., Raphael, M.N., Cartwright, J., Klekociuk, A.R., Wang, Z., Porter-Smith, R., 2021. Eighteen-year record of circum-Antarctic landfast-sea-ice distribution allows detailed baseline characterisation and reveals trends and variability. Cryosphere 15 (11), 5061–5077. https://doi.org/10.5194/tc-15-5061-2021.

Fraser, A.D., Wongpan, P., Langhorne, P.J., Klekociuk, A.R., Kusahara, K., Lannuzel, D., Massom, R.A., Meiners, K.M., Swadling, K.M., Atwater, D.P., Brett, G.M., Corkill, M., Dalman, L.A., Fiddes, S., Granata, A., Guglielmo, L., Heil, P., Leonard, G.H., Mahoney, A.R., McMinn, A., van der Merwe, P., Weldrick, C.K., Wienecke, B., 2023. Antarctic Landfast Sea ice: a review of its physics, biogeochemistry and ecology. Rev. Geophys. 61 (2) https://doi.org/10.1029/2022RG000770 e2022RG000770.

Friedlingstein, P., O'Sullivan, M., Jones, M.W., Andrew, R.M., Gregor, L., Hauck, J., Le Quéré, C., Luijkx, I.T., Olsen, A., Peters, G.P., Peters, W., Pongratz, J., Schwingshackl, C., Sitch, S., Canadell, J.G., Ciais, P., Jackson, R.B., Alin, S.R., Alkama, R., Arneth, A., Arora, V.K., Bates, N.R., Becker, M., Bellouin, N., Bittig, H.C., Bopp, L., Chevallier, F., Chini, L.P., Cronin, M., Evans, W., Falk, S., Feely, R.A., Gasser, T., Gehlen, M., Gkritzalis, T., Gloege, L., Grassi, G., Gruber, N., Gürses, Ö., Harris, I., Hefner, M., Houghton, R.A., Hurtt, G.C., Iida, Y., Ilyina, T., Jain, A.K., Jersild, A., Kadono, K., Kato, E., Kennedy, D., Klein Goldewijk, K., Knauer, J., Korsbakken, J.I., Landschützer, P., Lefèvre, N., Lindsay, K., Liu, J., Liu, Z., Marland, G., Mayot, N., McGrath, M.J., Metzl, N., Monacci, N.M., Munro, D.R., Nakaoka, S.I., Niwa, Y., O'Brien, K., Ono, T., Palmer, P.I., Pan, N., Pierrot, D., Pocock, K., Poulter, B., Resplandy, L., Robertson, E., Rödenbeck, C., Rodriguez, C., Rosan, T.M., Schwinger, J., Séférian, R., Shutler, J.D., Skjelvan, I., Steinhoff, T., Sun, Q., Sutton, A.J., Sweeney, C., Takao, S., Tanhua, T., Tans, P.P., Tian, X., Tian, H., Tilbrook, B., Tsujino, H., Tubiello, F., van der Werf, G.R., Walker, A.P., Wanninkhof, R., Whitehead, C., Willstrand Wranne, A., Wright, R., Yuan, W., Yue, C., Yue, X., Zaehle, S., Zeng, J., Zheng, B., 2022. Global Carbon Budget 2022. Earth Syst. Sci. Data 14 (11), 4811–4900. https://doi.org/10.5194/essd-14-4811-2022.

Fripiat, F., Cardinal, D., Tison, J.-L., Worby, A., André, L., 2007. Diatom-induced silicon isotopic fractionation in Antarctic Sea ice. J. Geophys. Res. Biogeosci. 112 (G2) https://doi.org/10.1029/2006JG000244.

Fripiat, F., Sigman, D.M., Fawcett, S.E., Rafter, P.A., Weigand, M.A., Tison, J.L., 2014a. New insights into sea ice nitrogen biogeochemical dynamics from the nitrogen isotopes. Glob. Biogeochem. Cycles 28 (2), 115–130. https://doi.org/10.1002/2013gb004729.

Fripiat, F., Tison, J.-L., André, L., Notz, D., Delille, B., 2014b. Biogenic silica recycling in sea ice inferred from Si-isotopes: constraints from Arctic winter first-year sea ice. Biogeochemistry 119 (1), 25–33. https://doi.org/10.1007/s10533-013-9911-8.

Fripiat, F., Sigman, D.M., Masse, G., Tison, J.L., 2015. High turnover rates indicated by changes in the fixed N forms and their stable isotopes in Antarctic landfast sea ice. J. Geophys. Res. Oceans 120 (4), 3079–3097. https://doi.org/10.1002/2014jc010583.

Fripiat, F., Meiners, K.M., Vancoppenolle, M., Papadimitriou, S., Thomas, D.N., Ackley, S.F., Arrigo, K.R., Carnat, G., Cozzi, S., Delille, B., Dieckmann, G.S., Dunbar, R.B., Fransson, A., Kattner, G., Kennedy, H., Lannuzel, D., Munro, D.R., Nomura, D., Rintala, J.M., Schoemann, V., Stefels, J., Steiner, N., Tison, J.L., 2017. Macro-nutrient concentrations in Antarctic pack ice: overall patterns and overlooked processes. Elementa-Sci. Anthropocene 5. https://doi.org/10.1525/elementa.217.

Fripiat, F., Declercq, M., Sapart, C.J., Anderson, L.G., Bruechert, V., Deman, F., Fonseca-Batista, D., Humborg, C., Roukaerts, A., Semiletov, I.P., Dehairs, F., 2018. Influence of the bordering shelves on nutrient distribution in the Arctic halocline inferred from water column nitrate isotopes. Limnol. Oceanogr. 63 (5), 2154–2170. https://doi.org/10.1002/lno.10930.

Fripiat, F., Martínez-García, A., Marconi, D., Fawcett, S.E., Kopf, S.H., Luu, V.H., Rafter, P.A., Zhang, R., Sigman, D.M., Haug, G.H., 2021. Nitrogen isotopic constraints on nutrient transport to the upper ocean. Nat. Geosci. 14 (11), 855–861. https://doi.org/10.1038/s41561-021-00836-8.

Frölicher, T.L., Sarmiento, J.L., Paynter, D.J., Dunne, J.P., Krasting, J.P., Winton, M., 2015. Dominance of the Southern Ocean in anthropogenic carbon and heat uptake in CMIP5 models. J. Clim. 28 (2), 862–886. https://doi.org/10.1175/JCLI-D-14-00117.1.

Gelaro, R., McCarty, W., Suárez, M.J., Todling, R., Molod, A., Takacs, L., Randles, C.A., Darmenov, A., Bosilovich, M.G., Reichle, R., Wargan, K., Coy, L., Cullather, R., Draper, C., Akella, S., Buchard, V., Conaty, A., da Silva, A.M., Gu, W., Kim, G.-K., Koster, R., Lucchesi, R., Merkova, D., Nielsen, J.E., Partyka, G., Pawson, S., Putman, W., Rienecker, M., Schubert, S.D., Sienkiewicz, M., Zhao, B., 2017. The modern-era retrospective analysis for research and applications, version 2 (MERRA-2). J. Clim. 30 (14), 5419–5454. https://doi.org/10.1175/JCLI-D-16-0758.1.

Gibson, J.A.E., Trull, T.W., 1999. Annual cycle of fCO2 under sea-ice and in open water in Prydz Bay, East Antarctica. Mar. Chem. 66 (3), 187–200. https://doi.org/10.1016/S0304-4203(99)00040-7.

Gillies, C.L., Stark, J.S., Johnstone, G.J., Smith, S.D.A., 2013. Establishing a food web model for coastal Antarctic benthic communities: a case study from the Vestfold Hills. Mar. Ecol. Prog. Ser. 478, 27–41. https://doi.org/10.3354/meps10214.

Gleitz, M., Thomas, D.N., 1993. Variation in phytoplankton standing stock, chemical composition and physiology during sea-ice formation in the southeastern Weddell Sea, Antarctica. J. Exp. Mar. Biol. Ecol. 173 (2), 211–230. https://doi.org/10.1016/0022-0981(93)90054-R.

Gleitz, M., Vonderloeff, M.R., Thomas, D.N., Dieckmann, G.S., Millero, F.J., 1995. Comparison of summer and winter inorganic carbon, oxygen and nutrient

concentrations in Antarctic Sea-ice brine. Mar. Chem. 51 (2), 81–91. https://doi.org/10.1016/0304-4203(95)00053-T.
Gleitz, M., Kukert, H., Riebesell, U., Dieckmann, G.S., 1996. Carbon acquisition and growth of Antarctic Sea ice diatoms in closed bottle incubations. Mar. Ecol. Prog. Ser. 135 (1/3), 169–177. https://doi.org/10.3354/meps135169.
Gordon, A.L., 1981. Seasonality of Southern Ocean sea ice. J. Geophys. Res. Oceans 86 (C5), 4193–4197. https://doi.org/10.1029/JC086iC05p04193.
Gradinger, R., Ikavalko, J., 1998. Organism incorporation into newly forming Arctic Sea ice in the Greenland Sea. J. Plankton Res. 20 (5), 871–886. https://doi.org/10.1093/plankt/20.5.871.
Greenwood, J.E., Truesdale, V.W., Rendell, A.R., 2001. Biogenic silica dissolution in seawater — in vitro chemical kinetics. Prog. Oceanogr. 48 (1), 1–23. https://doi.org/10.1016/S0079-6611(00)00046-X.
Guglielmo, L., Carrada, G.C., Catalano, G., Cozzi, S., Dell'Anno, A., Fabiano, M., Granata, A., Lazzara, L., Lorenzelli, R., Manganaro, A., Mangoni, O., Misic, C., Modigh, M., Pusceddu, A., Saggiomo, V., 2004. Biogeochemistry and algal communities in the annual sea ice at Terra Nova Bay (Ross Sea, Antarctica). Chem. Ecol. 20 (sup1), 43–55. https://doi.org/10.1080/02757540310001656657.
Günther, S., Dieckmann, G.S., 1999. Seasonal development of algal biomass in snow-covered fast ice and the underlying platelet layer in the Weddell Sea, Antarctica. Antarct. Sci. 11 (3), 305–315. https://doi.org/10.1017/S0954102099000395.
Günther, S., Gleitz, M., Dieckmann, G., 1999. Biogeochemistry of Antarctic Sea ice: a case study on platelet ice layers at Drescher inlet, Weddell Sea. Mar. Ecol. Prog. Ser. 177, 1–13. https://doi.org/10.3354/meps177001.
Hartnett, H., Boehme, S., Thomas, C., DeMaster, D., Smith, C., 2008. Benthic oxygen fluxes and denitrification rates from high-resolution porewater profiles from the Western Antarctic peninsula continental shelf. Deep-Sea Res. II Top. Stud. Oceanogr. 55 (22), 2415–2424. https://doi.org/10.1016/j.dsr2.2008.06.002.
Heil, P., 2006. Atmospheric conditions and fast ice at Davis, East Antarctica: a case study. J. Geophys. Res. Oceans 111 (C5). https://doi.org/10.1029/2005JC002904.
Heil, P., Allison, I., Lytle, V.I., 1996. Seasonal and interannual variations of the oceanic heat flux under a landfast Antarctic Sea ice cover. J. Geophys. Res. Oceans 101 (C11), 25741–25752. https://doi.org/10.1029/96JC01921.
Henley, S.F., Tuerena, R.E., Annett, A.L., Fallick, A.E., Meredith, M.P., Venables, H.J., Clarke, A., Ganeshram, R.S., 2017. Macronutrient supply, uptake and recycling in the coastal ocean of the West Antarctic peninsula. Deep-Sea Res. Part Ii-Top. Stud. Oceanogr. 139, 58–76. https://doi.org/10.1016/j.dsr2.2016.10.003.
Henley, S.F., Jones, E.M., Venables, H.J., Meredith, M.P., Firing, Y.L., Dittrich, R., Heiser, S., Stefels, J., Dougans, J., 2018. Macronutrient and carbon supply, uptake and cycling across the Antarctic peninsula shelf during summer. Philos. Trans. R. Soc. A Math. Phys. Eng. Sci. 376 (2122) https://doi.org/10.1098/rsta.2017.0168.
Henley, S.F., Cavan, E.L., Fawcett, S.E., Kerr, R., Monteiro, T., Sherrell, R.M., Bowie, A. R., Boyd, P.W., Barnes, D.K.A., Schloss, I.R., Marshall, T., Flynn, R., Smith, S., 2020. Changing biogeochemistry of the Southern Ocean and its ecosystem implications. Front. Mar. Sci. 7 https://doi.org/10.3389/fmars.2020.00581.
Holmes, R.M., Aminot, A., Kerouel, R., Hooker, B.A., Peterson, B.J., 1999. A simple and precise method for measuring ammonium in marine and freshwater ecosystems. Can. J. Fish. Aquat. Sci. 56 (10), 1801–1808. https://doi.org/10.1139/cjfas-56-10-1801.
Hoppmann, M., Richter, M.E., Smith, I.J., Jendersie, S., Langhorne, P.J., Thomas, D.N., Dieckmann, G.S., 2020. Platelet ice, the Southern Ocean's hidden ice: a review. Ann. Glaciol. 61 (83), 341–368. https://doi.org/10.1017/aog.2020.54.
Horner, R., Ackley, S.F., Dieckmann, G.S., Gulliksen, B., Hoshiai, T., Legendre, L., Melnikov, I.A., Reeburgh, W.S., Spindler, M., Sullivan, C.W., 1992. Ecology of sea ice biota .1. Habitat, terminology, and methodology. Polar Biol. 12 (3–4), 417–427.
Hu, Y.-B., Dieckmann, G.S., Wolf-Gladrow, D.A., Nehrke, G., 2014. Laboratory study on coprecipitation of phosphate with ikaite in sea ice. J. Geophys. Res. Oceans 119 (10), 7007–7015. https://doi.org/10.1002/2014JC010079.
Hydes, D.J., Aoyama, M., Aminot, A., Bakker, K., Becker, S., Coverly, S., Daniel, A., Dickson, A.G., Grosso, O., Kerouel, R., van Ooijen, J., Sato, K., Tanhua, T., Woodward, E.M.S., Zhang, J.Z., 2010. Determination of dissolved nutrients (N, P, SI) in seawater with high precision and inter-comparability using gas-segmented continuous flow analysers. In: Hood, E.M., Sabine, C.L., Sloyan, B.M. (Eds.), The GO-SHIP Repeat Hydrography Manual: A Collection of Expert Reports and Guidelines. Version 1. https://doi.org/10.25607/OBP-15 (Vol. IOCCP Report Number 14).
Ichinomiya, M., Honda, M., Shimoda, H., Saito, K., Odate, T., Fukuchi, M., Taniguchi, A., 2007. Structure of the summer under fast ice microbial community near Syowa Station, eastern Antarctica. Polar Biol. 30 (10), 1285–1293. https://doi.org/10.1007/s00300-007-0289-8.
Inall, M.E., Brearley, J.A., Henley, S.F., Fraser, A.D., Reed, S., 2022. Landfast ice controls on turbulence in Antarctic coastal seas. J. Geophys. Res. Oceans 127 (1). https://doi.org/10.1029/2021JC017963 e2021JC017963.
Janssens, J., Meiners, K.M., Tison, J.-L., Dieckmann, G., Delille, B., Lannuzel, D., 2016. Incorporation of iron and organic matter into young Antarctic Sea ice during its initial growth stages. Elementa: Sci. Anthropocene 4, 000123. https://doi.org/10.12952/journal.elementa.000123.
Jones, E.M., Henley, S.F., van Leeuwe, M.A., Stefels, J., Meredith, M.P., Fenton, M., Venables, H.J., 2022. Carbon and nutrient cycling in Antarctic landfast sea ice from winter to summer. Limnol. Oceanogr. https://doi.org/10.1002/lno.12260.
Kattner, G., 1999. Storage of dissolved inorganic nutrients in seawater: poisoning with mercuric chloride. Mar. Chem. 67 (1), 61–66. https://doi.org/10.1016/S0304-4203(99)00049-3.
Kawamura, T., Ohshima, K.I., Takizawa, T., Ushio, S., 1997. Physical, structural, and isotopic characteristics and growth processes of fast sea ice in Lützow-Holm Bay, Antarctica. J. Geophys. Res. Oceans 102 (C2), 3345–3355. https://doi.org/10.1029/96JC03206.
Klausmeier, C.A., Litchman, E., Daufresne, T., Levin, S.A., 2004. Optimal nitrogen-to-phosphorus stoichiometry of phytoplankton. Nature 429 (6988), 171–174. https://doi.org/10.1038/nature02454.
Kokare, C.R., Chakraborty, S., Khopade, A.N., Mahadik, K.R., 2009. Biofilm: importance and applications. Indian J. Biotechnol. 8, 159–168.
Kristiansen, S., Farbrot, T., Kuosa, H., Myklestad, S., von Quillfeldt, C.H., 1998. Nitrogen uptake in the infiltration community, an ice algal community in Antarctic pack-ice. Polar Biol. 19, 307–315. https://doi.org/10.1007/s003000050251.
Lannuzel, D., Bowie, A.R., Remenyi, T., Lam, P., Townsend, A., Ibisanmi, E., Butler, E., Wagener, T., Schoemann, V., 2011. Distributions of dissolved and particulate iron in the sub-Antarctic and polar frontal Southern Ocean (Australian sector). Deep-Sea Res. II Top. Stud. Oceanogr. 58 (21), 2094–2112. https://doi.org/10.1016/j.dsr2.2011.05.027.
Lannuzel, D., van der Merwe, P.C., Townsend, A.T., Bowie, A.R., 2014. Size fractionation of iron, manganese and aluminium in Antarctic fast ice reveals a lithogenic origin and low iron solubility. Mar. Chem. 161, 47–56. https://doi.org/10.1016/j.marchem.2014.02.006.
Lannuzel, D., Chever, F., van der Merwe, P.C., Janssens, J., Roukaerts, A., Cavagna, A.-J., Townsend, A.T., Bowie, A.R., Meiners, K.M., 2016a. Iron biogeochemistry in Antarctic pack ice during SIPEX-2. Deep-Sea Res. II Top. Stud. Oceanogr. 131, 111–122. https://doi.org/10.1016/j.dsr2.2014.12.003.
Lannuzel, D., Vancoppenolle, M., van der Merwe, P., de Jong, J., Meiners, K.M., Grotti, M., Nishioka, J., Schoemann, V., 2016b. Iron in sea ice: review and new insights. Elementa: Sci. Anthropocene 4, 000130. https://doi.org/10.12952/journal.elementa.000130.
Lei, R., Li, Z., Cheng, B., Zhang, Z., Heil, P., 2010. Annual cycle of landfast sea ice in Prydz Bay, East Antarctica. J. Geophys. Res. Oceans 115 (C2). https://doi.org/10.1029/2008JC005223.
Letscher, R.T., Moore, J.K., 2015. Preferential remineralization of dissolved organic phosphorus and non-Redfield DOM dynamics in the global ocean: impacts on marine productivity, nitrogen fixation, and carbon export. Glob. Biogeochem. Cycles 29 (3), 325–340. https://doi.org/10.1002/2014GB004904.
Li, X., Shokr, M., Hui, F., Chi, Z., Heil, P., Chen, Z., Yu, Y., Zhai, M., Cheng, X., 2020. The spatio-temporal patterns of landfast ice in Antarctica during 2006–2011 and 2016–2017 using high-resolution SAR imagery. Remote Sens. Environ. 242, 111736 https://doi.org/10.1016/j.rse.2020.111736.
Lieblappen, R.M., Kumar, D.D., Pauls, S.D., Obbard, R.W., 2018. A network model for characterizing brine channels in sea ice. Cryosphere 12 (3), 1013–1026. https://doi.org/10.5194/tc-12-1013-2018.
Lieser, J.L., Curran, M.A.J., Bowie, A.R., Davidson, A.T., Doust, S.J., Fraser, A.D., Galton-Fenzi, B.K., Massom, R.A., Meiners, K.M., Melbourne-Thomas, J., Reid, P.A., Strutton, P.G., Vance, T.R., Vancoppenolle, M., Westwood, K.J., Wright, S.W., 2015. Antarctic slush-ice algal accumulation not quantified through conventional satellite imagery: beware the ice of march. Cryosphere Discuss 2015, 6187–6222. https://doi.org/10.5194/tcd-9-6187-2015.
Lim, S.M., Moreau, S., Vancoppenolle, M., Deman, F., Roukaerts, A., Meiners, K.M., Janssens, J., Lannuzel, D., 2019. Field observations and physical-biogeochemical Modeling suggest low silicon affinity for Antarctic fast ice diatoms. J. Geophys. Res. Oceans 124 (11), 7837–7853. https://doi.org/10.1029/2018JC014458.
Lizotte, M.P., Sullivan, C.W., 1992. Biochemical composition and photosynthate distribution in sea ice microalgae of McMurdo Sound, Antarctica: evidence for nutrient stress during the spring bloom. Antarct. Sci. 4 (1), 23–30. https://doi.org/10.1017/S0954102092000063.
Loh, A.N., Bauer, J.E., 2000. Distribution, partitioning and fluxes of dissolved and particulate organic C, N and P in the eastern North Pacific and southern oceans. Deep-Sea Res. I Oceanogr. Res. Pap. 47 (12), 2287–2316. https://doi.org/10.1016/S0967-0637(00)00027-3.
Macdonald, R.W., McLaughlin, F.A., Wong, C.S., 1986. The storage of reactive silicate samples by freezing. Limnol. Oceanogr. 31 (5), 1139–1142. https://doi.org/10.4319/lo.1986.31.5.1139.
Maksym, T., Jeffries, M.O., 2000. A one-dimensional percolation model of flooding and snow ice formation on Antarctic Sea ice. J. Geophys. Res. Oceans 105 (C11), 26313–26331. https://doi.org/10.1029/2000JC900130.
Maranger, R., Pullin, M.J., 2003. 8 - elemental complexation by dissolved organic matter in lakes: Implications for Fe speciation and the speciation and the bioavailability of Fe and P. In: Findlay, S.E.G., Sinsabaugh, R.L. (Eds.), Aquatic Ecosystems. Academic Press, Burlington, pp. 185–214. https://doi.org/10.1016/B978-012256371-3/50009-3. ISBN: 978-0-12-256371-3.
Marshall, J., Speer, K., 2012. Closure of the meridional overturning circulation through Southern Ocean upwelling. Nat. Geosci. 5 (3), 171–180. https://doi.org/10.1038/ngeo1391.
Martin-Jézéquel, V., Hildebrand, M., Brzezinski, M.A., 2000. Silicon metabolism in diatoms: implications for growth. J. Phycol. 36 (5), 821–840. https://doi.org/10.1046/j.1529-8817.2000.00019.x.
Massom, R.A., Giles, A.B., Fricker, H.A., Warner, R.C., Legresy, B., Hyland, G., Young, N., Fraser, A.D., 2010. Examining the interaction between multi-year landfast sea ice and the Mertz glacier tongue, East Antarctica: another factor in ice sheet stability? J. Geophys. Res. Oceans 115. https://doi.org/10.1029/2009jc006083.
Maykut, G.A., Untersteiner, N., 1971. Some results from a time-dependent thermodynamic model of sea ice. J. Geophys. Res. (1896–1977) 76 (6), 1550–1575. https://doi.org/10.1029/JC076i006p01550.
McGuinness, M.J., Williams, M.J.M., Langhorne, P.J., Purdie, C., Crook, J., 2009. Frazil deposition under growing sea ice. J. Geophys. Res. Oceans 114 (C7). https://doi.org/10.1029/2007JC004414.

McMinn, A., Skerratt, J., Trull, T., Ashworth, C., Lizotte, M., 1999. Nutrient stress gradient in the bottom 5cm of fast ice, McMurdo Sound, Antarctica. Polar Biol. 21 (4), 220–227. https://doi.org/10.1007/s003000050356.

Meiners, K.M., Michel, C., 2017. Dynamics of nutrients, dissolved organic matter and exopolymers in sea ice. In: Thomas, D.N. (Ed.), Sea Ice, Third edition. Wiley-Blackwell, Oxford, U.K, pp. 415–432. https://doi.org/10.1002/9781118778371.ch17. ISBN: 9781118778371.

Meiners, K., Krembs, C., Gradinger, R., 2008. Exopolymer particles: microbial hotspots of enhanced bacterial activity in Arctic fast ice (Chukchi Sea). Aquat. Microb. Ecol. 52, 195–207. https://doi.org/10.3354/ame01214.

Meiners, K.M., Vancoppenolle, M., Thanassekos, S., Dieckmann, G.S., Thomas, D.N., Tison, J.L., Arrigo, K.R., Garrison, D.L., McMinn, A., Lannuzel, D., van der Merwe, P., Swadling, K.M., Smith Jr., W.O., Melnikov, I., Raymond, B., 2012. Chlorophyll a in Antarctic Sea ice from historical ice core data. Geophys. Res. Lett. 39 (21) https://doi.org/10.1029/2012GL053478.

Meiners, K.M., Vancoppenolle, M., Carnat, G., Castellani, G., Delille, B., Delille, D., Dieckmann, G.S., Flores, H., Fripiat, F., Grotti, M., Lange, B.A., Lannuzel, D., Martin, A., McMinn, A., Nomura, D., Peeken, I., Rivaro, P., Ryan, K.G., Stefels, J., Swadling, K.M., Thomas, D.N., Tison, J.L., van der Merwe, P., van Leeuwe, M.A., Weldrick, C., Yang, E.J., 2018. Chlorophyll-a in Antarctic Landfast Sea ice: a first synthesis of historical ice Core data. J. Geophys. Res. Oceans 123 (11), 8444–8459. https://doi.org/10.1029/2018JC014245.

Mills, M.M., Brown, Z.W., Laney, S.R., Ortega-Retuerta, E., Lowry, K.E., van Dijken, G.L., Arrigo, K.R., 2018. Nitrogen limitation of the summer phytoplankton and heterotrophic prokaryote communities in the Chukchi Sea. Front. Mar. Sci. 5 https://doi.org/10.3389/fmars.2018.00362. UNSP 362.

Moore, C.M., Mills, M.M., Arrigo, K.R., Berman-Frank, I., Bopp, L., Boyd, P.W., Galbraith, E.D., Geider, R.J., Guieu, C., Jaccard, S.L., Jickells, T.D., La Roche, J., Lenton, T.M., Mahowald, N.M., Maranon, E., Marinov, I., Moore, J.K., Nakatsuka, T., Oschlies, A., Saito, M.A., Thingstad, T.F., Tsuda, A., Ulloa, O., 2013. Processes and patterns of oceanic nutrient limitation. Nat. Geosci. 6 (9), 701–710. https://doi.org/10.1038/Ngeo1765.

Moore, J.K., Fu, W.W., Primeau, F., Britten, G.L., Lindsay, K., Long, M., Doney, S.C., Mahowald, N., Hoffman, F., Randerson, J.T., 2018. Sustained climate warming drives declining marine biological productivity. Science 359 (6380), 1139–1142. https://doi.org/10.1126/science.aao6379.

Moreau, S., Vancoppenolle, M., Delille, B., Tison, J.-L., Zhou, J., Kotovitch, M., Thomas, D.N., Geilfus, N.-X., Goosse, H., 2015. Drivers of inorganic carbon dynamics in first-year sea ice: a model study. J. Geophys. Res. Oceans 120 (1), 471–495. https://doi.org/10.1002/2014JC010388.

Moreau, S., Lannuzel, D., Janssens, J., Arroyo, M.C., Corkill, M., Cougnon, E., Genovese, C., Legresy, B., Lenton, A., Puigcorbé, V., Ratnarajah, L., Rintoul, S., Roca-Martí, M., Rosenberg, M., Shadwick, E.H., Silvano, A., Strutton, P.G., Tilbrook, B., 2019. Sea ice meltwater and circumpolar deep water drive contrasting productivity in three Antarctic polynyas. J. Geophys. Res. Oceans 124 (5), 2943–2968. https://doi.org/10.1029/2019JC015071.

Mortenson, E., Hayashida, H., Steiner, N., Monahan, A., Blais, M., Gale, M.A., Galindo, V., Gosselin, M., Hu, X., Lavoie, D., Mundy, C.J., 2017. A model-based analysis of physical and biological controls on ice algal and pelagic primary production in resolute passage. Elementa: Sci. Anthropocene 5, 39. https://doi.org/10.1525/elementa.229.

Murphy, E.J., Clarke, A., Symon, C., Priddle, J., 1995. Temporal variation in Antarctic Sea-ice: analysis of a long term fast-ice record from the South Orkney Islands. Deep-Sea Res. I Oceanogr. Res. Pap. 42 (7), 1045–1062. https://doi.org/10.1016/0967-0637(95)00057-D.

Nelson, D.M., Tréguer, P., 1992. Role of silicon as a limiting nutrient to Antarctic diatoms: evidence from kinetic studies in the Ross Sea ice-edge zone. Mar. Ecol.-Prog. Ser. 80, 255–264. https://doi.org/10.3354/meps080255.

Nelson, D.M., Ahern, J.A., Herlihy, L.J., 1991. Cycling of biogenic silica within the upper water column of the Ross Sea. Mar. Chem. 35 (1), 461–476. https://doi.org/10.1016/S0304-4203(09)90037-8.

Nelson, D.M., Brzezinski, M.A., Sigmon, D.E., Franck, V.M., 2001. A seasonal progression of Si limitation in the Pacific sector of the Southern Ocean. Deep-Sea Res. II Top. Stud. Oceanogr. 48 (19), 3973–3995. https://doi.org/10.1016/S0967-0645(01)00076-5.

Nomura, D., Koga, S., Kasamatsu, N., Shinagawa, H., Simizu, D., Wada, M., Fukuchi, M., 2012. Direct measurements of DMS flux from Antarctic fast sea ice to the atmosphere by a chamber technique. J. Geophys. Res. Oceans 117 (C4). https://doi.org/10.1029/2010JC006755.

Nomura, D., Aoki, S., Simizu, D., Iida, T., 2018. Influence of sea ice crack formation on the spatial distribution of nutrients and microalgae in flooded Antarctic multiyear ice. J. Geophys. Res. Oceans 123 (2), 939–951. https://doi.org/10.1002/2017JC012941.

Nowak, A., Hodson, A., Turchyn, A.V., 2018. Spatial and temporal dynamics of dissolved organic carbon, chlorophyll, nutrients, and trace metals in maritime Antarctic snow and snowmelt. Front. Earth Sci. 6 https://doi.org/10.3389/feart.2018.00201.

Orr, J.C., Maier-Reimer, E., Mikolajewicz, U., Monfray, P., Sarmiento, J.L., Toggweiler, J. R., Taylor, N.K., Palmer, J., Gruber, N., Sabine, C.L., Le Quere, C., Key, R.M., Boutin, J., 2001. Estimates of anthropogenic carbon uptake from four three-dimensional global ocean models. Glob. Biogeochem. Cycles 15 (1), 43–60. https://doi.org/10.1029/2000gb001273.

Papadimitriou, S., Kennedy, H., Kennedy, P., Thomas, D.N., 2013. Ikaite solubility in seawater-derived brines at 1atm and sub-zero temperatures to 265K. Geochim. Cosmochim. Acta 109, 241–253. https://doi.org/10.1016/j.gca.2013.01.044.

Parkinson, C.L., 2019. A 40-y record reveals gradual Antarctic Sea ice increases followed by decreases at rates far exceeding the rates seen in the Arctic. Proc. Natl. Acad. Sci. 116 (29), 14414–14423. https://doi.org/10.1073/pnas.1906556116.

Paterson, H., Laybourn-Parry, J., 2012. Sea ice microbial dynamics over an annual ice cycle in Prydz Bay, Antarctica. Polar Biol. 35 (7), 993–1002. https://doi.org/10.1007/s00300-011-1146-3.

Pellichero, V., Sallée, J.-B., Schmidtko, S., Roquet, F., Charrassin, J.-B., 2017. The ocean mixed layer under Southern Ocean sea-ice: seasonal cycle and forcing. J. Geophys. Res. Oceans 122 (2), 1608–1633. https://doi.org/10.1002/2016JC011970.

Pellichero, V., Sallée, J.-B., Chapman, C.C., Downes, S.M., 2018. The southern ocean meridional overturning in the sea-ice sector is driven by freshwater fluxes. Nat. Commun. 9 (1), 1789. https://doi.org/10.1038/s41467-018-04101-2.

Pieńkowski, A.J., Marret, F., Thomas, D.N., Scourse, J.D., Dieckmann, G.S., 2009. Dinoflagellates in a fast-ice covered inlet of the Riiser-Larsen ice shelf (Weddell Sea). Polar Biol. 32 (9), 1331–1343. https://doi.org/10.1007/s00300-009-0630-5.

Priscu, J.C., Sullivan, C.W., 1998. Nitrogen metabolism in Antarctic fastice microalgal assemblages. In: Lizotte, M., Arrigo, K. (Eds.), Antarctic Sea Ice Biological Processes, Interactions and Variability. American Geophysical Union, pp. 147–160. Vol. Antarctic Research Series 73,. ISBN: 978-1-118-66814-6.

Priscu, J.C., Downes, M.T., Priscu, L.R., Palmisano, A.C., Sullivan, C.W., 1990. Dynamics of ammonium oxidizer activity and nitrous oxide (N_2O) within and beneath Antarctic Sea ice. Mar. Ecol. Prog. Ser. 62 (1/2), 37–46.

Rees Jones, D.W., Wells, A.J., 2018. Frazil-ice growth rate and dynamics in mixed layers and sub-ice-shelf plumes. Cryosphere 12 (1), 25–38. https://doi.org/10.5194/tc-12-25-2018.

Reigstad, M., Wassmann, P., Wexels Riser, C., Øygarden, S., Rey, F., 2002. Variations in hydrography, nutrients and chlorophyll a in the marginal ice-zone and the Central Barents Sea. J. Mar. Syst. 38, 9–29. https://doi.org/10.1016/S0924-7963(02)00167-7.

Riaux-Gobin, C., Poulin, M., Prodon, R., Treguer, P., 2003. Land-fast ice microalgal and phytoplanktonic communities (Adélie land, Antarctica) in relation to environmental factors during ice break-up. Antarct. Sci. 15 (3), 353–364. https://doi.org/10.1017/S0954102003001378.

Riaux-Gobin, C., Dieckmann, G.S., Poulin, M., Neveux, J., Labrune, C., Vétion, G., 2013. Environmental conditions, particle flux and sympagic microalgal succession in spring before the sea-ice break-up in Adélie land, East Antarctica. Polar Res. 32 (0) https://doi.org/10.3402/polar.v32i0.19675.

Richter, O., Gwyther, D.E., King, M.A., Galton-Fenzi, B.K., 2022. The impact of tides on Antarctic ice shelf melting. Cryosphere 16 (4), 1409–1429. https://doi.org/10.5194/tc-16-1409-2022.

Roukaerts, A., Cavagna, A.J., Fripiat, F., Lannuzel, D., Meiners, K.M., Dehairs, F., 2016. Sea-ice algal primary production and nitrogen uptake rates off East Antarctica. Deep-Sea Res. Part Ii-Top. Stud. Oceanogr. 131, 140–149. https://doi.org/10.1016/j.dsr2.2015.08.007.

Roukaerts, A., Nomura, D., Deman, F., Hattori, H., Dehairs, F., Fripiat, F., 2019. The effect of melting treatments on the assessment of biomass and nutrients in sea ice (Saroma-ko lagoon, Hokkaido, Japan). Polar Biol. 42 (2), 347–356. https://doi.org/10.1007/s00300-018-2426-y.

Roukaerts, A., Deman, F., Van der Linden, F., Carnat, G., Bratkic, A., Moreau, S., Lannuzel, D., Dehairs, F., Delille, B., Tison, J.-L., Fripiat, F., 2021. The biogeochemical role of a microbial biofilm in sea ice: Antarctic landfast sea ice as a case study. Elementa: Sci. Anthropocene 9 (1), 00134. https://doi.org/10.1525/elementa.2020.00134.

Rusciano, E., Budillon, G., Fusco, G., Spezie, G., 2013. Evidence of atmosphere–sea ice–ocean coupling in the Terra Nova Bay polynya (Ross Sea—Antarctica). Cont. Shelf Res. 61-62, 112–124. https://doi.org/10.1016/j.csr.2013.04.002.

Rysgaard, S., Wang, F., Galley, R.J., Grimm, R., Notz, D., Lemes, M., Geilfus, N.X., Chaulk, A., Hare, A.A., Crabeck, O., Else, B.G.T., Campbell, K., Sørensen, L.L., Sievers, J., Papakyriakou, T., 2014. Temporal dynamics of ikaite in experimental sea ice. Cryosphere 8 (4), 1469–1478. https://doi.org/10.5194/tc-8-1469-2014.

Saenz, B.T., Arrigo, K.R., 2012. Simulation of a sea ice ecosystem using a hybrid model for slush layer desalination. J. Geophys. Res. Oceans 117. https://doi.org/10.1029/2011jc007544.

Saenz, B.T., Arrigo, K.R., 2014. Annual primary production in Antarctic Sea ice during 2005–2006 from a sea ice state estimate. J. Geophys. Res. Oceans 119 (6), 3645–3678. https://doi.org/10.1002/2013JC009677.

Saggiomo, M., Poulin, M., Mangoni, O., Lazzara, L., De Stefano, M., Sarno, D., Zingone, A., 2017. Spring-time dynamics of diatom communities in landfast and underlying platelet ice in Terra Nova Bay, Ross Sea, Antarctica. J. Mar. Syst. 166, 26–36. https://doi.org/10.1016/j.jmarsys.2016.06.007.

Sahashi, R., Nomura, D., Toyota, T., Tozawa, M., Ito, M., Wongpan, P., Ono, K., Simizu, D., Naoki, K., Nosaka, Y., Tamura, T., Aoki, S., Ushio, S., 2022. Effects of snow and remineralization processes on nutrient distributions in multi-year Antarctic Landfast Sea ice. J. Geophys. Res. Oceans 127 (7). https://doi.org/10.1029/2021JC018371 e2021JC018371.

Sakamoto, C.M., Friederich, G.E., Codispoti, L.A., 1990. MBARI Procedures for Automated Nutrient Analyses Using a Modified Alpkem Series 300 Rapid Flow Analyzer. Monterey Bay Aquarium Research Institute.

Sarmiento, J.L., Gruber, N., Brzezinski, M.A., Dunne, J.P., 2004. High-latitude controls of thermocline nutrients and low latitude biological productivity. Nature 427 (6969), 56–60. https://doi.org/10.1038/nature02127.

Sarthou, G., Timmermans, K.R., Blain, S., Tréguer, P., 2005. Growth physiology and fate of diatoms in the ocean: a review. J. Sea Res. 53 (1), 25–42. https://doi.org/10.1016/j.seares.2004.01.007.

Schnack-Schiel, S.B., Thomas, D.N., Haas, C., Dieckmann, G.S., Alheit, R., 2001. The occurrence of the copepods Stephos longipes (Calanoida) and Drescheriella glacialis

(Harpacticoida) in summer sea ice in the Weddell Sea, Antarctica. Antarct. Sci. 13 (2), 150–157. https://doi.org/10.1017/S0954102001000232.
Stapleford, L.S., Smith, R.E.H., 1996. The interactive effects of temperature and silicon limitation on the psychrophilic ice diatom Pseudonitszchia seriata. Polar Biol. 16, 589–594. https://doi.org/10.1007/BF02329056.
Stief, P., Schauberger, C., Lund, M.B., Greve, A., Abed, R.M.M., Al-Najjar, M.A.A., Attard, K., Bonaglia, S., Deutzmann, J.S., Franco-Cisterna, B., García-Robledo, E., Holtappels, M., John, U., Maciute, A., Magee, M.J., Pors, R., Santl-Temkiv, T., Scherwass, A., Sevilgen, D.S., de Beer, D., Glud, R.N., Schramm, A., Kamp, A., 2022. Intracellular nitrate storage by diatoms can be an important nitrogen pool in freshwater and marine ecosystems. Commun. Earth Environ. 3 (1), 154. https://doi.org/10.1038/s43247-022-00485-8.
Sturm, M., Massom, R.A., 2009. Snow and sea ice. In: Thomas, D.N. (Ed.), Sea Ice, Second edition. Wiley-Blackwell, Oxford, U.K, pp. 153–204. https://doi.org/10.1002/9781444317145.ch5. ISBN: 9781444317145.
Sturm, M., Massom, R.A., 2017. Snow in the sea ice system: Friend or foe? In: Thomas, D. N. (Ed.), Sea Ice, Third edition. Wiley-Blackwell, Oxford, U.K, pp. 65–109. https://doi.org/10.1002/9781118778371.ch3. ISBN: 9781118778371.
Sun, S., Hattermann, T., Pattyn, F., Nicholls, K.W., Drews, R., Berger, S., 2019. Topographic shelf waves control seasonal melting near Antarctic ice shelf grounding lines. Geophys. Res. Lett. 46 (16), 9824–9832. https://doi.org/10.1029/2019GL083881.
Swadling, K.M., Constable, A.J., Fraser, A.D., Massom, R.A., Borup, M.D., Ghigliotti, L., Granata, A., Guglielmo, L., Johnston, N.M., Kawaguchi, S., Kennedy, F., Kiko, R., Koubbi, P., Makabe, R., Martin, A., McMinn, A., Moteki, M., Pakhomov, E.A., Peeken, I., Reimer, J., Reid, P., Ryan, K.G., Vacchi, M., Virtue, P., Weldrick, C.K., Wongpan, P., Wotherspoon, S.J., 2023. Biological responses to change in Antarctic sea ice habitats. Front. Ecol. Evol. 10, 1073823 https://doi.org/10.3389/fevo.2022.1073823.
Tang, S., Qin, D., Ren, J., Kang, J., Li, Z., 2007. Structure, salinity and isotopic composition of multi-year landfast sea ice in Nella Fjord, Antarctica. Cold Reg. Sci. Technol. 49 (2), 170–177. https://doi.org/10.1016/j.coldregions.2007.03.005.
Thomas, D.N., Dieckmann, G.S., 2002. Biogeochemistry of Antarctic Sea ice. In: Gibson, R.N., Barnes, M., Atkinson, R.J.A. (Eds.), Oceanography and Marine Biology: An Annual Review, vol. 40. Taylor and Francis, pp. 143–169.
Thomas, D.N., Lara, R.J., Haas, C.J., Schnack-Schiel, S.B., Dieckmann, G.S., Kattner, G., Nöthig, E.-M.S., Mizdalski, E.S., 1998. Biological soup within decaying summer sea ice in the Amundsen Sea, Antarctica. In: Antarctic Sea Ice: Biological Processes, Interactions and Variability, pp. 161–171. ISBN: 9781118668146. https://doi.org/10.1029/AR073p0161.
Thomas, D.N., Kennedy, H., Kattner, G., Gerdes, D., Gough, C., Dieckmann, G.S., 2001. Biogeochemistry of platelet ice: its influence on particle flux under fast ice in the Weddell Sea, Antarctica. Polar Biol. 24 (7), 486–496. https://doi.org/10.1007/s003000100243.
Thrush, S., Dayton, P., Cattaneo-Vietti, R., Chiantore, M., Cummings, V., Andrew, N., Hawes, I., Kim, S., Kvitek, R., Schwarz, A.-M., 2006. Broad-scale factors influencing the biodiversity of coastal benthic communities of the Ross Sea. Deep-Sea Res. II Top. Stud. Oceanogr. 53 (8), 959–971. https://doi.org/10.1016/j.dsr2.2006.02.006.
Tison, J.L., Worby, A., Delille, B., Brabant, F., Papadimitriou, S., Thomas, D., de Jong, J., Lannuzel, D., Haas, C., 2008. Temporal evolution of decaying summer first-year sea ice in the Western Weddell Sea, Antarctica. Deep-Sea Res. II Top. Stud. Oceanogr. 55 (8), 975–987. https://doi.org/10.1016/j.dsr2.2007.12.021.
Tison, J.L., Schwegmann, S., Dieckmann, G., Rintala, J.M., Meyer, H., Moreau, S., Vancoppenolle, M., Nomura, D., Engberg, S., Blomster, L.J., Hendricks, S., Uhlig, C., Luhtanen, A.M., de Jong, J., Janssens, J., Carnat, G., Zhou, J., Delille, B., 2017. Biogeochemical impact of snow cover and cyclonic intrusions on the winter Weddell Sea ice pack. J. Geophys. Res. Oceans 122 (12), 9548–9571. https://doi.org/10.1002/2017JC013288.
Torstensson, A., Dinasquet, J., Chierici, M., Fransson, A., Riemann, L., Wulff, A., 2015. Physicochemical control of bacterial and protist community composition and diversity in Antarctic Sea ice. Environ. Microbiol. 17 (10), 3869–3881. https://doi.org/10.1111/1462-2920.12865.
Toyota, T., Massom, R., Lecomte, O., Nomura, D., Heil, P., Tamura, T., Fraser, A.D., 2016. On the extraordinary snow on the sea ice off East Antarctica in late winter, 2012. Deep-Sea Res. II Top. Stud. Oceanogr. 131, 53–67. https://doi.org/10.1016/j.dsr2.2016.02.003.
Tremblay, J.E., Anderson, L.G., Matrai, P., Coupel, P., Belanger, S., Michel, C., Reigstad, M., 2015. Global and regional drivers of nutrient supply, primary production and CO2 drawdown in the changing Arctic Ocean. Prog. Oceanogr. 139, 171–196. https://doi.org/10.1016/j.pocean.2015.08.009.
Underwood, G., Fietz, S., Papadimitriou, S., Thomas, D., Dieckmann, G., 2010. Distribution and composition of dissolved extracellular polymeric substances (EPS) in Antarctic Sea ice. Mar. Ecol.-Prog. Ser. 404, 1–19. https://doi.org/10.3354/meps08557.
United States National Snow and Ice Data Center, 2023. Sea Ice Data and Analysis Tools. https://nsidc.org/arcticseaicenews/sea-ice-tools/. Accessed 10/05/2023.
van der Merwe, P., Lannuzel, D., Bowie, A.R., Meiners, K.M., 2011. High temporal resolution observations of spring fast ice melt and seawater iron enrichment in East Antarctica. J. Geophys. Res. Biogeosci. 116 (G3) https://doi.org/10.1029/2010JG001628.
van Leeuwe, M.A., Tedesco, L., Arrigo, K.R., Assmy, P., Campbell, K., Meiners, K.M., Rintala, J.M., Selz, V., Thomas, D.N., Stefels, J., 2018. Microalgal community structure and primary production in Arctic and Antarctic Sea ice: a synthesis. Elementa-Sci. Anthropocene 6. https://doi.org/10.1525/elementa.267.
van Leeuwe, M.A., Fenton, M., Davey, E., Rintala, J.-M., Jones, E.M., Meredith, M.P., Stefels, J., 2022. On the phenology and seeding potential of sea-ice microalgal species. Elementa: Sci. Anthropocene 10 (1), 00029. https://doi.org/10.1525/elementa.2021.00029.
Vancoppenolle, M., Goosse, H., de Montety, A., Fichefet, T., Tremblay, B., Tison, J.-L., 2010. Modeling brine and nutrient dynamics in Antarctic Sea ice: the case of dissolved silica. J. Geophys. Res. Oceans 115 (C2). https://doi.org/10.1029/2009JC005369.
Vancoppenolle, M., Meiners, K.M., Michel, C., Bopp, L., Brabant, F., Carnat, G., Delille, B., Lannuzel, D., Madec, G., Moreau, S., Tison, J.-L., van der Merwe, P., 2013. Role of sea ice in global biogeochemical cycles: emerging views and challenges. Quat. Sci. Rev. 79, 207–230. https://doi.org/10.1016/j.quascirev.2013.04.011.
Yuan, G., Lavkulich, L.M., 1994. Phosphate sorption in relation to extractable iron and Aluminum in Spodosols. Soil Sci. Soc. Am. J. 58 (2), 343–346. https://doi.org/10.2136/sssaj1994.03615995005800020013x.
Zhang, R., Zheng, M., Chen, M., Ma, Q., Cao, J., Qiu, Y., 2014. An isotopic perspective on the correlation of surface ocean carbon dynamics and sea ice melting in Prydz Bay (Antarctica) during austral summer. Deep-Sea Res. I Oceanogr. Res. Pap. 83, 24–33. https://doi.org/10.1016/j.dsr.2013.08.006.
Zhou, M., Rhue, R.D., Harris, W.G., 1997. Phosphorus sorption characteristics of Bh and Bt horizons from Sandy coastal plain soils. Soil Sci. Soc. Am. J. 61 (5), 1364–1369. https://doi.org/10.2136/sssaj1997.03615995006100050011x.